IMPROVED MODE MATCHING METHOD FOR SCATTERING FROM LARGE CAVITIES

By

Weiwei Zhang

A DISSERTATION

Submitted to
Michigan State University
in partial fulfillment of the requirements
for the degree of

DOCTOR OF PHILOSOPHY

Department of Mathematics

2006

ABSTRACT

IMPROVED MODE MATCHING METHOD FOR SCATTERING FROM LARGE CAVITIES

By

Weiwei Zhang

The accurate calculations of electromagnetic fields play a crucial role in aircraft design and antenna design. The methods proposed in the literature for the EM fields calculation of scattering from large cavities are not be fast, accurate and easily implemented enough.

In this dissertation, the calculations of EM fields for 2D large open cavities are considered first. By defining two extension operators, the exact solution and the mode matching solution may be formulated under the same framework, which makes it possible to analyze the difference. Using an asymptotic technique, we present a new (improved) mode matching method. In particular, the explicit solution and the error estimate are given. Numerical examples, including EM fields calculations and RCS calculations, are presented. The second part of the dissertation is about the calculations of EM fields for 3D cavities. Following the similar idea, mode matching method and improved mode matching method are presented. Numerical examples are showed to demonstrate the efficiency of the method.

ACKNOWLEDGMENTS

I wish to thank my advisor, Professor Gang Bao, for his encouragement, suggestions, and guidance during the time I worked on this dissertation. It would have been impossible for me to make this dissertation a reality without his sharing the knowledge and discussing various ideas throughout the study.

I wish to thank Professor Chichia Chiu, Professor Leo Kempel, Professor Baisheng Yan and Professor Zhengfang Zhou, in my thesis committee, for their suggestions, comments and help in my research and life.

I wish to thank my parents and my parents-in-law, for their enduring patience, constant support and encouragement.

I wish to thank my friends and all the people who have helped me.

Last but not least, I would like to give my thanks to my husband Yang and my son Max, for their love.

TABLE OF CONTENTS

LIST OF FIGURES

Introduction

0.1 Background and Motivation

A two dimensional open cavity recessed in an infinite ground plan can serve as a model of duct structures such as jet engine intakes of an aircraft or antenna windows embedded in complicated structures. The phenomena are governed by the Helmholtz equation in an infinite domain along with the radiation condition and Perfect Electric Conductor boundary conditions.

The prediction and reduction of Radar Cross Section (or echo area) of this structure are very important and require the information of the fields across a broad range of frequencies. For instance, a short wavelength radar (e.g. missile seekers) and a long wavelength radar (e.g. early warning radar) may both exist at the same time. Thus the accurate calculation of electromagnetic fields is of great importance. When the cavity parameters are small or the frequency is relatively low, a large body of work such as finite element methods, integral equations or hybrid methods have been done [8], [12], [13]. For a large cavity or at high frequencies, the calculation of the fields becomes difficult. I. Babuska pointed out that, for a model problem, the Galerkin solution differs significantly from the best approximation with increasing the wave number. A. K. Aziz showed that "k^2h is small" is the sufficient condition to guarantee that the error of the Galerkin solution has the same magnitude as the error of the best approximation, where k is the wave number and h is the mesh size.

Another major difficulty of the problem is that the mathematical formulations of cavity problems always involve nonlocal boundary conditions and singular integrals [8], [3]. Physically, large cavities involve a large amount of internal reflections.

In the engineering literature, modal methods have been adopted to calculate electromagnetic fields at high frequencies or for large cavities because of their efficiency and accuracy [9], [11]. To the best of knowledge, in these methods, the boundary condition at infinity is approximated from some physical intuitions or assumptions and confirmed by numerical experiments in some cases. However, without rigorous error estimates, there is no guarantee that the numerical simulations are correct.

In this work, the time harmonic plane wave incidence is considered. The ground plane and the walls of the open cavity are perfect electric conductors and the cavity is filled with magnetic or nonmagnetic layered medium. A bounded domain problem is set up by using Fourier transform, the radiation condition and the continuity condition. The mode matching solution $v(x,y)$ and the exact solution $u(x,y)$ are formulated under the same framework by applying zero extension E_0 and periodic extension E_P on the transparent operator T, i.e.

$$\frac{\partial u(x,0)}{\partial y} + g(x) = T(E_0(u(x,0))),$$
$$\frac{\partial v(x,0)}{\partial y} + g(x) = T(E_P(v(x,0))).$$

In the case of simple geometries, the mode matching method is easily implemented. By analyzing the error between u and v, and applying some asymptotic techniques, an improved mode matching method is obtained. The new method provides an explicit solution which converges to the exact one at the rate of $O(1/\sqrt{w})$, where w is the width of the cavity. Due to the error control, the method is expected to be extremely useful for large dimensions or high wavenumber cavity problems. Numerical experiments of the electromagnetic fields in the aperture and different Radar Cross Section calculations have been studied.

The existence and uniqueness of the partial differential equation were proved by Ammari, Bao and Wood in [3] for the case when $\Im\epsilon > 0$. In this dissertation, a TM case result for $\Im\epsilon < -1/k_0^2$ is given.

In three dimensional case, the governing equations are Maxwell's equations. The application includes metallic cavities RCS study, and electromagnetic penetration and transmission properties of objects consisting of these substructures. It has great importance in industries, including telecommunication, engine and antenna manufacturing. Besides the same difficulties from two dimensional large open cavity problems, the computational time and memory requirements are sometimes intolerably large. Therefore, the three dimensional cavity problem has been regarded as a grand challenging problem for decades. In the literature, eddy elements, discrete Galerkin methods, integral equations and modal methods were applied to calculate Radar Cross Section[8]. But none of them are fast, accurate and easily implemented at the same time.

In this dissertation, the continuity conditions, Silver-Mueller Radiation condition and Fourier transform are used to derive the exact PDE model in a bounded region. Numerical experiments are studied.

This work could be easily generalized to other applications, such as scattering and transmission through the slot in a conducting plane. Following the idea, open cavity problem with a canonical shape could be solve similarly using different field expansions. For example, the spherical harmonics.

0.2 Organization

In Chapter 1, the two dimensional cavity problem is mainly discussed. The mathematical formulation, including the Helmholtz equation, boundary conditions, weak formulation are introduced in section 1. The well-posedness of the variational problem is further established for the TM case, when $\Im(\epsilon) < -1/k_0^2$ in section 2. In section 3, the mode matching method is introduced by using a periodic extension operator. The idea and fulfillment of improved mode matching method are discussed in section 4. And the convergence analysis is given in this section as well. The numerical experiments are displayed in section 5.

Chapter 2 is focused on 3d open cavity problem. The continuity conditions and Maxwell's equations are introduced in section 1. In section 2, the field representation based on sine or cosine functions are given. The fulfillment of the mode matching method is given in section 3. Some numerical examples using the mode matching method are shown as well. In section 4, the improved mode matching method is proposed following the idea in 2d case. In section 5, the benchmarks in the literature are studied.

Appendix displays some results about the integral involving $\sin(wx)/x$. When the considered function is relatively smooth, the numerical simulations of the integrals are studied in term of a Dirac Delta function.

CHAPTER 1

TWO DIMENSIONAL CAVITY PROBLEM

1.1 Preliminaries

Consider an open cavity recessed in an infinite ground plane (see Figure 1.1). The ground plane and cavity walls are perfect electric conductors (PEC) and the cavity is invariant along Z direction. The time harmonic electromagnetic fields (time dependence $e^{-i\omega t}$) satisfy the Maxwell's equations

$$\nabla \times E - i\omega\mu H = 0,$$

$$\nabla \times H + i\omega\epsilon E = 0,$$

where E and H are the electric and magnetic fields, respectively. Assume the media inside the cavity are not perfect dielectrics and have finite conductivity.

In this case the continuity conditions on the open aperture Γ are

$$\hat{z} \times (E_0 - E_1) = 0$$

$$\hat{z} \times (H_0 - H_1) = 0$$

$$\hat{z} \cdot (D_0 - D_1) = \rho_S$$

$$\hat{z} \cdot (B_0 - B_1) = J_s$$

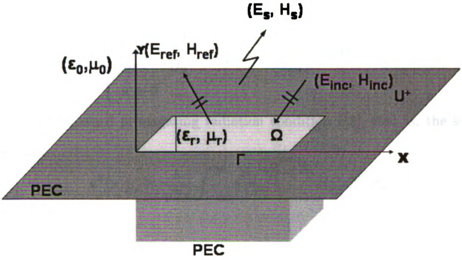

Figure 1.1. Three dimensional open cavity.

where ρ_S, J_S are the surface charge density and surface current density, D and B are the electric and magnetic flux [16]. Here subscript 0 denotes the quantities above the cavity and subscript 1 denotes the quantities inside the cavity.

In the case of the TM polarization, the electric field is parallel to the z-axis. Therefore the electric field has the following form,

$$E = \begin{cases} E_0 = (0,0,u_0) & \text{in } U^+, \\ E_1 = (0,0,u) & \text{in } \Omega. \end{cases}$$

Let u^i, u^r, u^s be the z component of the incident field, reflective field and scattering field in U^+, respectively. Let $k_i = k_0\sqrt{\epsilon_i \mu_i}$ $(i = 0, 1)$ be the wave numbers above and below the ground plane, respectively. Then

$$\begin{cases} \dfrac{\partial^2 u_0}{\partial x^2} + \dfrac{\partial^2 u_0}{\partial y^2} + k_0^2 u_0 = 0 & \text{in } U^+, \\ \dfrac{\partial^2 u}{\partial x^2} + \dfrac{\partial^2 u}{\partial y^2} + k_1^2 u = 0 & \text{in } \Omega, \\ u = 0 & \text{on PEC }, \end{cases} \tag{1.1}$$

along with the upward propagating radiation condition [15], that is, the scattering field satisfies

$$u^s(x,y) = \frac{i}{\sqrt{2\pi}} \int_{-\infty}^{\infty} e^{i\sqrt{k_0^2-\xi^2}y} \hat{\phi}(\xi) e^{i\xi x} d\xi. \tag{1.2}$$

where $\phi(x) = u_0|_{y=0}$.

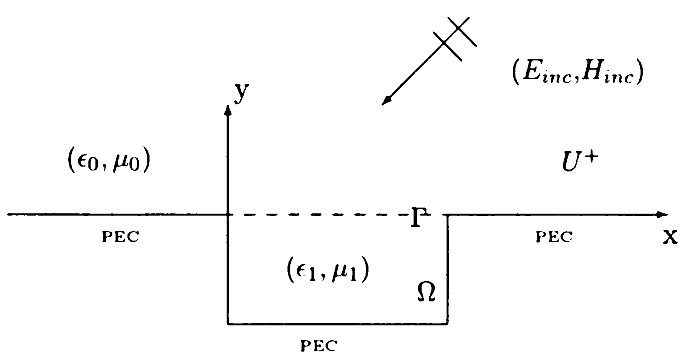

Figure 1.2. Two dimensional open cavity

It is clear that $u_0 = u^i + u^r + u^s$ above the ground. By assuming a plane wave incidence with the incident angle θ_i (with respect to the y axis), the continuity conditions then read

$$\begin{aligned} &u^s(x,0) = u(x,0) \qquad x \in [0, w], \\ &\mu_1 \frac{\partial u^s}{\partial y}(x,0) - \mu_0 \frac{\partial u}{\partial y}(x,0) = g(x) \qquad x \in [0, w], \end{aligned} \tag{1.3}$$

where $g(x) = -2i\mu_1 k_0 \cos\theta_i e^{-ik_0 x \sin\theta_i}$ and w is the width of the cavity.

Obviously, above is a problem in an unbounded domain $U^+ \cup \Omega$. Next, the continuity condition is used to derive an equivalent form in the bounded domain Ω. For convenience, the transparent operator T is defined [12] and the zero extension operator E_0 as

$$T(v) = \frac{i}{\sqrt{2\pi}} \int_{-\infty}^{\infty} \sqrt{k_0^2 - \xi^2} \hat{v}(\xi) e^{i\xi x} d\xi, \tag{1.4}$$

$$E_0(v(x)) = \begin{cases} v(x) & x \in [0, w], \\ 0 & \text{otherwise}, \end{cases} \tag{1.5}$$

Here $\hat{v}$ is the Fourier transform of v.

Taking the Fourier transform with respect to x of the Helmholtz equation in (1.1) and solving an ODE for y, a transparent boundary condition is easily derived [12] as

$$\frac{\partial u^s(x,0)}{\partial y} = T(E_0(u^s(x,0))). \tag{1.6}$$

Using the continuity conditions (1.3), the exact solution of (1.1) and (1.2) satisfies

$$\begin{cases} \dfrac{\partial^2 u}{\partial x^2} + \dfrac{\partial^2 u}{\partial y^2} + k_1^2 u = 0 & \text{in } \Omega, \\ u = 0 & \text{on PEC walls ,} \\ \mu_0 \dfrac{\partial u(x,0)}{\partial y} + g(x) = \mu_1 T(E_0(u(x,0))) & \text{on } \Gamma. \end{cases} \tag{1.7}$$

The weak formulation of the problem is : Find $u \in V$ (a suitable subspace of $H^1(\Omega)$ [12]) such that

$$a(u,v) = (g,v), \forall v \in V \tag{1.8}$$

where the bilinear form is defined by

$$a(u,v) = \int_\Omega \nabla u \cdot \overline{\nabla v} - \int_\Omega k_1^2 u \bar{v} - \int_\Gamma T(E_0(u(x,0))\bar{v}$$

and the well-posedness of the scattering problem was established in [3] and stated as the following Lemma:

Lemma 1.1.1. *If $\epsilon \in L^{\infty}(\Omega)$, $\Re(\epsilon) \geq \epsilon_1 > 0$ and $\Im(\epsilon) \geq 0$, the scattering problem (1.8) attains a unique solution in $H_0^1(\Omega)$.*

In the case of the TE polarization, the magnetic field is parallel to z-axis. Assume the z component of the magnetic field in the cavity is u. It satisfies

$$\begin{cases} \nabla \cdot (\frac{1}{\epsilon_1}\nabla u) + k_0^2 u = 0 & \text{in } \Omega, \\ \frac{\partial u}{\partial n} = 0 & \text{on PEC walls,} \\ u = S(E_0(\frac{\partial u}{\partial n})) + 2e^{ik_0 x \sin\theta_i} & \text{on } \Gamma \end{cases} \tag{1.9}$$

where

$$S(f) := \frac{1}{i\sqrt{2\pi}} \int_{-\infty}^{\infty} \frac{1}{\sqrt{k^2 - \xi^2}} \hat{f}(\xi) e^{i\xi x} d\xi$$

Here the cavity is considered non magnetic. The variational form of (1.9) is to find $u \in V$ (a suitable subspace of $H^1(\Omega)$ [12]) such that such that,

$$b(u, v) = \int_{\Gamma} q\bar{v}dx, \forall v \in V \tag{1.10}$$

where

$$b(u, v) = \int_{\Omega} \frac{1}{\epsilon_1} \nabla u \cdot \nabla \bar{v} dx dy - k^2 \int_{\Omega} u \cdot \bar{v} dx dy - \int_{\Gamma} \frac{1}{\epsilon_1} \frac{\partial u}{\partial n} \overline{S(E_0(\frac{\partial u}{\partial n}))} dx$$

and the well-posedness of the TE case was stated as follow [3]:

Lemma 1.1.2. *If $\epsilon \in L^{\infty}(\Omega)$, $\Re(\epsilon) \geq \epsilon_1 > 0$, $\Im(\epsilon) \geq 0$ and $\epsilon(x)$ is smooth enough (satisfies assumption (A) in [3]), the scattering problem (2.5) attains a unique solution in $H^1(\Omega)$.*

1.2 TM Case

Following the fractional Sobolev space notation as in [18], (adopt a wave number dependent norm, equivalent to the usual norm), the norm $|| \cdot ||_{H^s}$ is defined by

$$||u||_s^2 = \int (k_0^2 + \xi^2)^s |\hat{u}|^2 d\xi$$

In this case, it can be proved that $T \circ E_0$ is a bounded operator from $H^{1/2}$ to $H^{-1/2}$ and satisfies

$$||T \circ E_0|| \le 1.$$

Theorem 1.2.1. *Let $\epsilon_1 = \epsilon_{re} + i\epsilon_{im}$. Then the variational problem (1.7) has a unique solution in V if $\epsilon_{im} \in (-\infty, -1/k_0^2) \cup [0, \infty)$.*

Proof. When $\epsilon_{im} \ge 0$, the uniqueness of the problem was proved in [3]. Therefore the only one needed to prove is the case when $\epsilon_{im} \le -1/k_0^2$. From the definition,

$$\text{Im } a(u,u) = -\int_\Omega k_0^2 \epsilon_{im} |u|^2 dxdy - \int_{|\xi|<k_0} \sqrt{k_0^2 - \xi^2} |E_0(u)\hat{}|^2 d\xi$$

By Im $a(u,u) = 0$,

$$-\int_\Omega k_0^2 \epsilon_{im} |u|^2 dxdy = \int_{|\xi|<k_0} \sqrt{k_0^2 - \xi^2} |E_0(u)\hat{}|^2 d\xi \le ||T(E_0(u)|| ||u||_2 \le ||u||^2$$

Therefore when $\epsilon_{im} < -1/k_0^2$, $||u||_2 = 0$ is derived.

The existence follows from the Fredholm alternative. □

Notice that T is not a Hermitian operator, the uniqueness is not trivial for $\epsilon_2 \neq 0$.

Different bases, for example, piecewise polynomials, could be adopted to solve this model. In this dissertation, only the trigonometric bases are considered.

By the PEC condition, the exact solutions u consistent with (1.7) may be expanded as

$$u(x,y) = \sum_{n=1}^{\infty} a_n \sin(\frac{n\pi x}{w}) \sinh(\gamma_n (y+d)), \tag{2.11}$$

where d is the depth of the cavity, w is the width of the cavity and

$$\gamma_n = \sqrt{(n\pi/w)^2 - k_0^2 \mu_1 \epsilon_1}.$$

It is easy to derive the coefficients of the *sine* series of $g(x)$. It is given by

$$g_n = ik_0[1-(-1)^n e^{-ik_0 w\sin(\theta_i)}]\frac{2n\pi\cos(\theta_i)}{(n\pi)^2-(k_0 w\sin(\theta_i))^2}. \tag{2.12}$$

A direct Fourier transform calculation yields

$$(E_0\sin(\frac{n\pi}{w}\cdot))^{\frown}(\xi) = \frac{1}{\sqrt{2\pi}}\frac{-n\pi}{w}\left(\frac{1-(-1)^n e^{-iw\xi}}{\xi^2-(\frac{n\pi}{w})^2}\right). \tag{2.13}$$

Here $f(\cdot)^{\frown}(\xi) = \frac{1}{\sqrt{2\pi}}\int f(x)e^{-ix\xi}d\xi$.

1.3 Mode Matching Method

For large cavities, because of the large number of internal reflections, the exact solution is highly oscillatory. In order to calculate the solution more efficiency, an approximate model of (1.7) is considered first by using the periodic extension E_p. Define

$$E_p(v(x)) = \begin{cases} v(x) & x\in[0,w], \\ v(x-(n-1)w) & x\in[(n-1)w, nw] \end{cases}$$

The approximate model satisfies

$$\begin{cases} \frac{\partial^2 v}{\partial x^2}+\frac{\partial^2 v}{\partial y^2}+k_1^2 v = 0 & \text{in } \Omega, \\ v = 0 & \text{on PEC walls }, \\ \mu_0\frac{\partial v(x,0)}{\partial y}+g(x) = \mu_1 T(E_p(v(x,0))) & \text{on } \Gamma. \end{cases} \tag{3.14}$$

In this model (3.14), only the periodic extension is involved.

Similar as (2.11), the approximate solution v may be expanded as

$$v(x,y) = \sum_{n=1}^{\infty} b_n\sin(\frac{n\pi x}{w})\sinh(\gamma_n(y+d)). \tag{3.15}$$

and it is easily seen that

$$(E_p\sin(\frac{n\pi}{w}\cdot))^{\frown}(\xi) = \frac{i\pi}{\sqrt{2\pi}}(\delta(\xi+\frac{n\pi}{w})-\delta(\xi-\frac{n\pi}{w})), \tag{3.16}$$

where $\delta(\cdot)$ is the Dirac delta function. Hence

$$T \circ E_p(\sin(\frac{n\pi x}{w})) = -\sin(\frac{n\pi x}{w})\nu_n,$$

where

$$\nu_n = i\sqrt{k_0^2 - (n\pi/w)^2}. \tag{3.17}$$

Then the solution satisfies (3.14) may be given by (3.15) with

$$b_n = \frac{2ik_0}{\mu_1\nu_n \sinh(\gamma_n d) + \mu_0\gamma_n \cosh(\gamma_n d)} g_n. \tag{3.18}$$

It is clear to see that b_n decreases exponentially as n increases. This is the so called mode matching solution.

Remark 1.3.1. *In [10], Morgan expanded the field in the local region above the aperture using upward propagating waveguide modes bounded by vertical walls and obtained the same formula. Here, the same mode matching formula is derived by an alternative approach based on the use of the periodic extension operator E_p.*

Next is focused on the convergence rate of the above series.

Lemma 1.3.1. *Let c_k be the Fourier coefficients of $f(x)$. Then $\sum_k c_k^2 k^{2m} < \infty$ if and only if $f \in H_p^m$.*

Theorem 1.3.1. *Let $v(x,y)$ be the mode matching solution of (3.14), then $v(x,0) \in H_0^1([0,w])$. Moreover,*

$$\sum_{n=[w/\pi]}^{\infty} (b_n \sinh(\gamma_n d))^2 = O(\frac{1}{w}), \tag{3.19}$$

$$\sum_{n=1}^{[w/\pi]-1} (\frac{n\pi}{w} b_n \sinh(\gamma_n d))^2 = O(\frac{1}{w}). \tag{3.20}$$

Proof. For simplicity, let's consider the case of empty cavity with incident angle $\theta_i = 0$. Notice that

$$\lim_{x\to 0} \quad \frac{\sinh(x)}{x(\sinh(x)+\cosh(x))} = 1$$
$$\lim_{x\to \infty} \quad \frac{\sinh(x)}{x(\sinh(x)+\cosh(x))} = \lim_{x\to\infty} \frac{1}{2x}$$

From (2.12) and (3.18),

$$b_n \sinh(\gamma_n d) = O(\frac{1}{n\pi\gamma_n}).$$

Therefore (3.19) and (3.20) are true.

For more general cases, if $n\pi >> w$

$$b_n \sinh(\gamma_n d) = O(\frac{w}{(n\pi)^2}).$$

and if $n\pi << w$

$$b_n \sinh(\gamma_n d) = O(\frac{n\pi}{w^2}).$$

The same estimates could be still derived. From Lemma 1.3.1, it is clear to see that $v(x, 0) \in H_0^{1+\delta}([0, w])$, for some $\delta > 0$. □

For a two-layered medium cavity problem, define the permittivity inside the cavity as

$$\epsilon_r(v(x)) = \begin{cases} \epsilon_1, & y \in [-d_1, 0], \\ \epsilon_2, & y \in [-d, -d_1]. \end{cases}$$

Expand the field inside the cavity by

$$\begin{aligned} u_1(x,y) &= \sum_{n=1}^{\infty} [c_n \sinh(\beta_n(y+d)) + d_n \cosh(\beta_n(y+d))] \sin(\frac{n\pi x}{w}), y \in [-d_1, 0], \\ u_2(x,y) &= \sum_{n=1}^{\infty} b_n \sin(\frac{n\pi x}{w}) \sinh(\gamma_n(y+d)), \qquad y \in [-d, -d_1]. \end{aligned}$$

where

$$\beta_n = \sqrt{(n\pi/w)^2 - k_0^2\mu_1\epsilon_1},$$
$$\gamma_n = \sqrt{(n\pi/w)^2 - k_0^2\mu_2\epsilon_2},$$

u_1 and u_2 are the upper and lower fields inside the cavity, respectively. Using the continuity conditions on the interface,

$$c_n[\mu_0 \cosh(\beta_n d)\beta_n - \mu_1 \sinh(\beta_n d)\nu_n]$$
$$+d_n[\mu_0 \sinh(\beta_n d)\beta_n - \mu_1 \cosh(\beta_n d)\nu_n] = -g_n, \tag{3.21}$$
$$c_n \sinh(\beta_n d_2) + d_n \cosh(\beta_n d_2) - b_n \sinh(\gamma_n d_2) = 0, \tag{3.22}$$
$$c_n \mu_2 \cosh(\beta_n d_2)\beta_n + d_n \mu_2 \sinh(\beta_n d_2)\beta_n - b_n \mu_1 \cosh(\gamma_n d_2)\gamma_n = 0. \tag{3.23}$$

Here the permeability μ is assumed a constant everywhere. By solving the above system, a mode matching solution for the two-layered medium cavity problem is easily derived. The same idea could be applied to a general multi-layered medium problem. If consider the TE cases or the medium is vertical layered, $\cos(\frac{n\pi x}{w})$ should be used in the field expansions rather than $\sin(\frac{n\pi x}{w})$. The mode matching solution is again easily derived.

1.4 Improved Mode Matching Method

In order to find the difference between the exact solution and the mode matching solution, the difference between two operators acting on one single mode is analyzed first, i.e.,

$$
\begin{aligned}
& T \circ E_0(\sin(\frac{n\pi x}{w})) - T \circ E_p(\sin(\frac{n\pi x}{w})) \\
= & \frac{i}{2\pi}\int_{-k_0}^{k_0} e^{ix\xi}\sqrt{k_0^2-\xi^2}\left[\frac{1}{2}(1-(-1)^n\cos(w\xi))(\frac{1}{\xi+\frac{n\pi}{w}}-\frac{1}{\xi-\frac{n\pi}{w}})\right]d\xi \\
+ & \frac{i}{2\pi}\int_{-\infty}^{-k_0}+\int_{k_0}^{\infty} e^{ix\xi}\sqrt{k_0^2-\xi^2}\left[\frac{1}{2}(1-(-1)^n\cos(w\xi))(\frac{1}{\xi+\frac{n\pi}{w}}-\frac{1}{\xi-\frac{n\pi}{w}})\right]d\xi \\
+ & \frac{i}{2\pi}\int_{-\infty}^{\infty} e^{ix\xi}\sqrt{k_0^2-\xi^2}\left[\frac{i}{2}\frac{\sin(w(\xi+\frac{n\pi}{w}))}{\xi+\frac{n\pi}{w}}-\frac{i}{2}\frac{\sin(w(\xi-\frac{n\pi}{w}))}{\xi-\frac{n\pi}{w}}\right. \\
& \left. -i\pi\delta(\xi+\frac{n\pi}{w})+i\pi\delta(\xi-\frac{n\pi}{w})\,\right]d\xi \\
\triangleq & \; I_1+I_2+I_3+I_4
\end{aligned} \tag{4.24}
$$

Before proving the main theorem, let us define $Si(x)$ and $Ci(x)$ be the sine integral and cosine integral respectively. They have the following definitions and the asymptotic expansions,

$$
\begin{aligned}
Si(x) &= \int_0^x \frac{\sin t}{t}dt = \frac{\pi}{2} - \int_x^\infty \frac{\sin t}{t}dt && (4.25)\\
Ci(x) &= \gamma + \ln x + \int_0^x \frac{\cos t - 1}{t}dt = -\int_x^\infty \frac{\sin t}{t}dt && (4.26)\\
Si(x) &= \frac{\pi}{2} - \frac{\cos x}{x}\sum_{n=0}^{\infty}\frac{(-1)^n(2n)!}{x^{2n}} - \frac{\sin x}{x^2}\sum_{n=0}^{\infty}\frac{(-1)^n(2n+1)!}{x^{2n}} && (4.27)\\
Ci(x) &= \frac{\sin x}{x}\sum_{n=0}^{\infty}\frac{(-1)^n(2n)!}{x^{2n}} - \frac{\cos x}{x^2}\sum_{n=0}^{\infty}\frac{(-1)^n(2n+1)!}{x^{2n}}. && (4.28)
\end{aligned}
$$

The graphs of them are shown in Figure 1.3.

Lemma 1.4.1. *For sine integral and cosine integral, the following estimates hold,*

$$
|Si(x) - \pi/2| \leq \frac{2}{x}, \quad |Ci(x)| \leq \frac{2}{x}. \tag{4.29}
$$

Proof. The estimates could be derived by integration by parts. □

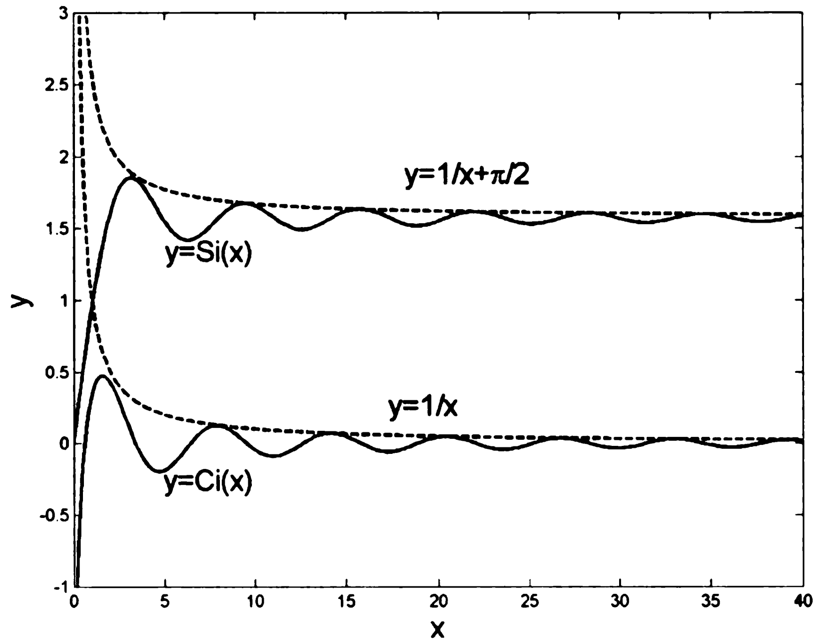

Figure 1.3. Sine integral and cosine integral.

The well known Riemann-Lebesgue Lemma says if $f \in L^1(R)$, then

$$\lim_{\epsilon \to 0} \int \sin(x/\epsilon) f(x) dx = 0,$$
$$\lim_{\epsilon \to 0} \int \cos(x/\epsilon) f(x) dx = 0.$$

The smoother the function $f(x)$ is, the faster the limit converges. But the integrands in I_2 and I_3 are not in L^1, it makes the analysis more challenging. N. Bleistein and ect. focused on log-like functions and established a generalized version of Riemann-Lebesgue Lemma [19]. Here in this work, an asymptotic expansion and anti-derivatives are used to prove the convergence. Again for the above limits, if $f(x)$ has singularity at $x = 0$,

$$\lim_{\epsilon \to 0} \sin(x/\epsilon) = \pi\delta(x)$$

should be used.

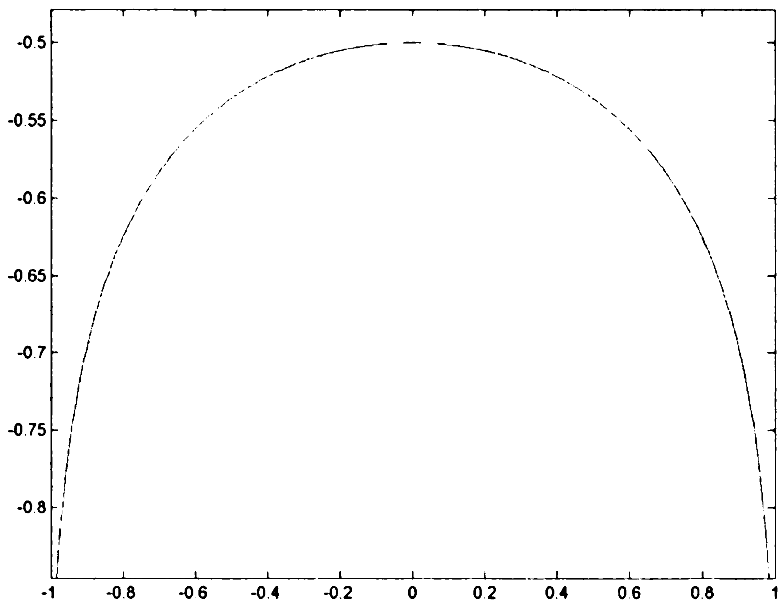

Figure 1.4. Graph of $r(x)$.

Lemma 1.4.2.

$$\int_{-1}^{1} \frac{\sin(\frac{x}{\epsilon})}{x}\sqrt{1-x^2}dx = \pi + O(\epsilon).$$

Proof. Define $f(x) = \sqrt{1-x^2}$, $x \in [-1,1]$. Because $f'(0) = 0$, therefore

$$f(x) = f(0) + x^2 r(x).$$

Here $r(x) = \dfrac{f(x) - f(0)}{x^2}$. It can be seen that $r'(x)$ has singularity at $x = 1$. Notice that

$$
\begin{aligned}
& \int_0^1 \frac{\sin(\frac{x}{\epsilon})}{x} f(x)dx & (4.30)\\
= \quad & f(0)Si(\frac{1}{\epsilon}) - \int_0^1 \sin(\frac{x}{\epsilon})xr(x)dx & (4.31)\\
= \quad & f(0)Si(\frac{1}{\epsilon}) - \epsilon\cos\frac{1}{\epsilon}r(1) - \epsilon\int_0^1 \cos(\frac{x}{\epsilon})\frac{d}{dx}(xr(x))dx & (4.32)\\
= \quad & \frac{\pi}{2} + O(\epsilon) - \epsilon\int_0^1 \cos(\frac{x}{\epsilon})\frac{d}{dx}(xr(x))dx & (4.33)
\end{aligned}
$$

Use the Riemann-Lebesgue Theorem in finite domain [a,b] and notice that $r(1) = -1$ and $xr(x)$ is a decreasing function on [-1,1].Therefore

$$\int_0^1 |\frac{d}{dx}(xr(x))|dx = -\int_0^1 \frac{d}{dx}(xr(x))dx = -xr(x)|_0^1 = 1.$$

Hence

$$\lim_{\epsilon\to 0}\int_0^1 \cos(\frac{x}{\epsilon})d(xr(x)) = 0$$

and

$$\int_{-1}^1 \frac{\sin(\frac{x}{\epsilon})}{x} f(x)dx = \pi + o(\epsilon).$$

□

Remark 1.4.1. *The above lemma in fact states that* $\lim_{\epsilon\to 0}\sin(x/\epsilon) = \pi\delta(x)$.

Remark 1.4.2. *For Riemann-Lebesgue Theorem, it could be further proved that if* $f(x)$ *is Lipschitz continuous on [a,b] , then*

$$\int_a^b \sin(x/\epsilon)f(x)dx = O(\epsilon),$$
$$\int_a^b \cos(x/\epsilon)f(x)dx = O(\epsilon)$$

(See Appendix). But $xr(x) \in L([0,1])$*, directly using Riemann-Lebesgue Theorem in (4.31) could just guarantee* $\lim_{\epsilon\to 0}\int_0^1 \sin(\frac{x}{\epsilon})xr(x)dx = 0$. *The first order convergent result could not be obtained. Also notice* $\frac{d}{dx}(xr(x))$ *has singularity at* $x = 1$*, the change of variable could not be used twice in (4.32) to get* ϵ^2 *term.*

Lemma 1.4.3. *If* $\frac{n\pi}{w} < 1$, *then for any* $a \in [0, w]$, *the following is true.*

$$\int_{-1}^{1} e^{iax}\sqrt{1-x^2}\left[\frac{\sin(w(x-\frac{n\pi}{w}))}{x-\frac{n\pi}{w}} - \frac{\sin(w(x+\frac{n\pi}{w}))}{x+\frac{n\pi}{w}}\right] dx$$
$$= \quad (Si(w-n\pi)+Si(w+n\pi))\sin(\frac{n\pi a}{w})\sqrt{1-(\frac{n\pi}{w})^2}+O(1/w).$$

Proof. Define

$$r_1(x,a) = \frac{\sin(ax)-\sin(\frac{n\pi a}{w})}{x-\frac{n\pi}{w}}$$
$$f_1(x,a) = \frac{\sqrt{1-x^2}-\sqrt{1-(\frac{n\pi}{w})^2}}{x-\frac{n\pi}{w}}$$
$$r_2(x,a) = \frac{\sin(ax)+\sin(\frac{n\pi a}{w})}{x+\frac{n\pi}{w}}$$
$$f_2(x,a) = \frac{\sqrt{1-x^2}-\sqrt{1-(\frac{n\pi}{w})^2}}{x+\frac{n\pi}{w}}$$

Then using the odd and even properties of the integrand,

$$
\begin{aligned}
&\frac{-i}{2}\int_{-1}^{1} e^{iax}\sqrt{1-x^2}\left[\frac{\sin(w(x-\frac{n\pi}{w}))}{x-\frac{n\pi}{w}}-\frac{\sin(w(x+\frac{n\pi}{w}))}{x+\frac{n\pi}{w}}\right]dx \\
=&\int_0^1 \sin(ax)\sqrt{1-x^2}\left[\frac{\sin(w(x-\frac{n\pi}{w}))}{x-\frac{n\pi}{w}}-\frac{\sin(w(x+\frac{n\pi}{w}))}{x+\frac{n\pi}{w}}\right]dx \\
=&\int_0^1 \sin(\frac{n\pi a}{w})\frac{\sin(w(x-\frac{n\pi}{w}))}{x-\frac{n\pi}{w}}\sqrt{1-(\frac{n\pi}{w})^2}dx \\
&+\int_0^1 r_1\sin(w(x-\frac{n\pi}{w}))\sqrt{1-(\frac{n\pi}{w})^2}dx \\
&+\int_0^1 \sin(\frac{n\pi a}{w})f_1\sin(w(x-\frac{n\pi}{w}))dx+\int_0^1 r_1f_1\sin(w(x-\frac{n\pi}{w}))(x-\frac{n\pi}{w})dx \\
&+\int_0^1 \sin(\frac{n\pi a}{w})\frac{\sin(w(x+\frac{n\pi}{w}))}{x+\frac{n\pi}{w}}\sqrt{1-(\frac{n\pi}{w})^2}dx \\
&-\int_0^1 r_2\sin(w(x+\frac{n\pi}{w}))\sqrt{1-(\frac{n\pi}{w})^2}dx \\
&+\int_0^1 \sin(\frac{n\pi a}{w})f_2\sin(w(x+\frac{n\pi}{w}))dx-\int_0^1 r_2f_2\sin(w(x+\frac{n\pi}{w}))(x+\frac{n\pi}{w})dx
\end{aligned}
$$

Similarly as in Lemma 1, the following facts could be proved:

First,

$$
\begin{aligned}
&\int_0^1 \frac{\sin(w(x-\frac{n\pi}{w}))}{x-\frac{n\pi}{w}}+\frac{\sin(w(x+\frac{n\pi}{w}))}{x+\frac{n\pi}{w}}dx \\
=&\int_{-n\pi}^{w-n\pi}\frac{\sin(x)}{x}dx+\int_{n\pi}^{w+n\pi}\frac{\sin(x)}{x}dx \\
=&\ Si(w-n\pi)+Si(w+n\pi)
\end{aligned}
$$

Second,

$$
\begin{aligned}
&\int_0^1 f_1\sin(w(x-\frac{n\pi}{w}))dx+\int_0^1 f_2\sin(w(x+\frac{n\pi}{w}))dx \\
=&\ (-1)^n\int_0^1\frac{2x(\sqrt{1-x^2}-\sqrt{1-(\frac{n\pi}{w})^2})}{x^2-(\frac{n\pi}{w})^2}\sin(wx)dx
\end{aligned}
$$

For convenience, the following definition is made: $F_1(x) = \dfrac{2x(\sqrt{1-x^2} - \sqrt{1-(\frac{n\pi}{w})^2})}{x^2 - (\frac{n\pi}{w})^2}$. It is a decreasing function and $\int_0^1 |F_1(x)|dx$ is finite. Therefore the above integral is $O(1/w)$.

Third,

$$
\begin{aligned}
& \int_0^1 r_1 \sin(w(x - \frac{n\pi}{w}))dx - \int_0^1 r_2 \sin(w(x + \frac{n\pi}{w}))dx \\
= & (-1)^n \int_0^1 \frac{2(\sin(ax)\frac{n\pi}{w} - x\sin(\frac{n\pi a}{w}))}{x^2 - (\frac{n\pi}{w})^2} \sin(wx)dx \\
= & O(\frac{1}{w})
\end{aligned}
$$

For simplicity, consider the case when $a = w$. The major contribution of the above integral is

$$
\begin{aligned}
& \int_0^1 \frac{(\sin(wx)^2\frac{n\pi}{w}}{x^2 - (\frac{n\pi}{w})^2} dx \\
= & \frac{1}{4}[log(t - n\pi) - log(t + n\pi) - Ci(2t - 2n\pi) + Ci(2t + 2n\pi)]_0^w = O(\frac{1}{w})
\end{aligned}
$$

Similar, the fourth conclusion is derived

$$
\begin{aligned}
& \int_0^1 r_1 f_1 \sin(w(x - \frac{n\pi}{w}))(x - \frac{n\pi}{w})dx - \int_0^1 r_2 f_2 \sin(w(x - \frac{n\pi}{w}))(x + \frac{n\pi}{w})dx \\
= & (-1)^n \int_0^1 \sin(wx)\frac{(\sin(ax) - \sin(\frac{n\pi a}{w}))(\sqrt{1-x^2} - \sqrt{1-(\frac{n\pi}{w})^2})}{(x - \frac{n\pi}{w})}dx = O(\frac{1}{w})
\end{aligned}
$$

□

Define $q_n = \int_{1/\epsilon}^{\infty} \frac{\sin(y)}{y^n}dy$, where $n \geq 1$. From (4.25), using the integration by parts, it could be easily proved that

$$
\begin{aligned}
q_n = & \epsilon^n [\cos\frac{1}{\epsilon} + n\epsilon\sin\frac{1}{\epsilon} - n(n+1)\epsilon^2\cos\frac{1}{\epsilon} - n(n+1)(n+2)\epsilon^3\sin\frac{1}{\epsilon}] \\
& + n(n+1)(n+2)(n+3)q_{n+4}, \qquad (4.34)
\end{aligned}
$$

and further more, $|q_{n+4}| = O(\epsilon^{n+3})$.

Lemma 1.4.4. *Assume $a = O(\epsilon^2)$, then*

$$\int_1^\infty \frac{\sin(\frac{x}{\epsilon})}{x^2 - a}\sqrt{x^2 - 1}dx = O(\epsilon).$$

Proof. Define $g(x) = \sqrt{1 - \frac{1}{x^2}}$, then $g(x) = f(\frac{1}{x})$ from the definition in Lemma 1.4.2. Use Taylor's expansion and (4.34),

$$\begin{aligned}
& \int_1^\infty \frac{\sin(\frac{x}{\epsilon})}{x^2 - a}\sqrt{x^2 - 1}dx \\
= & \int_1^\infty \sin(\frac{x}{\epsilon})(\frac{1}{x^2} + \frac{a}{x^4})\sqrt{x^2 - 1}dx + O(\epsilon^2) \\
= & \int_1^\infty \frac{\sin(\frac{x}{\epsilon})}{x}(f(0) - \frac{1}{x^2}r(\frac{1}{x}))dx + O(\epsilon^2) \\
= & \epsilon\cos(\frac{1}{\epsilon}) + o(\epsilon)
\end{aligned}$$

□

Lemma 1.4.5. *For any $a \in [0, w)$,*

$$\int_1^\infty + \int_{-\infty}^{-1} e^{iax}\sqrt{x^2 - 1}\left[\frac{\sin(w(x - \frac{n\pi}{w}))}{x - \frac{n\pi}{w}} - \frac{\sin(w(x + \frac{n\pi}{w}))}{x + \frac{n\pi}{w}}\right]dx = O(1/w).$$

Proof. Define $g(x) = \sqrt{\frac{1}{x^2} - 1}$, then $g(x) = f(\frac{1}{x})$ from the definition in Lemma

1.4.2. Use Taylor's expansion,

$$
\begin{aligned}
& \int_1^\infty + \int_{-\infty}^{-1} e^{iax}\sqrt{x^2-1}\left[\frac{\sin(w(x-\frac{n\pi}{w}))}{x-\frac{n\pi}{w}} - \frac{\sin(w(x+\frac{n\pi}{w}))}{x+\frac{n\pi}{w}}\right] dx \\
= \; & C\frac{n\pi}{w}\int_1^\infty \sin(ax)\frac{\sin(wx)}{x^2-(\frac{n\pi}{w})^2}\sqrt{x^2-1}dx \\
= \; & C\frac{n\pi}{w}\int_1^\infty \sin(ax)\sin(wx)(\frac{1}{x^2}+\frac{(\frac{n\pi}{w})^2}{x^4})\sqrt{x^2-1}dx + O((1/w)^2) \\
= \; & C\frac{n\pi}{w}\int_1^\infty \frac{\sin(ax)\sin(wx)}{x}(f(0)-\frac{1}{x^2}r(\frac{1}{x}))dx + O((1/w)^2) \\
= \; & C\frac{n\pi}{w}(Ci(w-a)-Ci(w+a)) + O((1/w)^2) \\
= \; & O(\frac{n\pi}{w})
\end{aligned}
$$

□

Remark 1.4.3. *If $\phi(x) \in C_0^\infty(R)$ is an even function, then*

$$
\begin{aligned}
& \frac{1}{\pi}\int_{-\infty}^\infty \frac{\sin(\frac{x}{\epsilon})}{x}\phi(x)dx \\
= \; & \int_{-\infty}^\infty \delta(x)\phi(x)dx + \epsilon^3\cos\frac{1}{\epsilon}\int_{-\infty}^\infty \delta(x)\phi^{(2)}(x)dx + O(\epsilon^4).
\end{aligned}
$$

In fact it provide us a way to correct the well known convergent result, $\lim_{w\to\infty}\frac{\sin(wx)}{x} = \pi\delta(x)$, to an arbitrary convergent rate in the sense of distribution (See Appendix). But in this work, since $\sqrt{1-x^2} \in C^{0,\frac{1}{2}}(R)$, the convergence rate degenerates to $O(\epsilon)$.

From the above lemmas,

$$
\left\{I_4 + \nu_n\left[\frac{Si(w-n\pi)+Si(w+n\pi)}{2\pi} - 1\right]\sin(\frac{n\pi x}{w})\right\} = O(\frac{n\pi}{w}),
$$

where ν_n is defined in (3.17).

For the second integral and the third integral in (4.24),

$$
\begin{aligned}
I_2 + I_3 &= \frac{i}{2\pi}\int_1^\infty \sqrt{1-\xi^2}(1-(-1)^n \cos w\xi k_0)\left(\frac{-2\frac{n\pi}{w}}{\xi^2-(\frac{n\pi}{wk_0})^2}\right)\cos(x\xi k_0)d\xi \\
&= \frac{i}{2\pi}\int_1^\infty (\xi - \frac{1}{2\xi} + O(\frac{1}{\xi^3}))(1-(-1)^n \cos w\xi k_0)\left(\frac{-2\frac{n\pi}{w}}{\xi^2-(\frac{n\pi}{wk_0})^2}\right)\cos(x\xi k_0)d\xi \\
&= \frac{i}{2\pi}\int_1^\infty \xi(1-(-1)^n \cos w\xi k_0)\left(\frac{-2\frac{n\pi}{w}}{\xi^2-(\frac{n\pi}{wk_0})^2}\right)\cos(x\xi k_0)d\xi + O(1/w)
\end{aligned}
$$

if $x \neq 0$. Now calculate

$$\int \xi(1-(-1)^n \cos w\xi k_0)\left(\frac{1}{\xi^2-(\frac{n\pi}{wk_0})^2}\right)\cos(x\xi k_0)d\xi.$$

Notice that the Lebesgue dominated convergence theorem could not be used due to the singularity of the kernel. When n is an even number, the anti derivative is,

$$
\begin{aligned}
AN(x) &= \sum_{k=1}^{2} \frac{(-1)^k}{2} Si(\frac{x(w\xi k_0 + (-1)^k n\pi)}{w})\sin(\frac{n\pi x}{w}) \\
&+ \sum_{k=1}^{2} \frac{1}{2} Ci(\frac{x(w\xi k_0 + (-1)^k n\pi)}{w})\cos(\frac{n\pi x}{w}) \\
&+ \sum_{m,k=1}^{2} \frac{(-1)^{m+1}}{4} Si(((-1)^k x + w)\frac{w\xi k_0 + (-1)^m n\pi}{w})\sin(n\pi\frac{(-1)^k x + w}{w}) \\
&+ \sum_{m,k=1}^{2} \frac{-1}{4} Ci(((-1)^k x + w)\frac{w\xi k_0 + (-1)^m n\pi}{w})\cos(n\pi\frac{(-1)^k x + w}{w})
\end{aligned}
$$

From Lemma 1.4.1,

$$I_2 + I_3 = \frac{i \cdot n}{w} Ci(k_0 x) + O(1/w) = O(\frac{n\pi}{w}).$$

A similar result could be derived for n which is an odd number. For the first integral,

$$
\begin{aligned}
I_1 &= \frac{i}{2\pi} \int_0^{k_0} \sqrt{k_0^2 - \xi^2}(1-(-1)^n \cos w\xi) \left(\frac{-2\frac{n\pi}{w}}{\xi^2 - (\frac{n\pi}{w})^2} \right) \cos(x\xi) d\xi \\
&= \frac{ik_0}{2\pi} \int_0^{k_0} (1-(-1)^n \cos w\xi) \left(\frac{-2\frac{n\pi}{w}}{\xi^2 - (\frac{n\pi}{w})^2} \right) \cos(x\xi) d\xi + O(\frac{n\pi}{w}).
\end{aligned}
$$

Evaluating the above definite integral,

$$
\left[I_1 - \frac{ik_0}{4\pi} f_n(x) \sin(\frac{n\pi x}{w}) \right] = O(\frac{n\pi}{w}) + R(x)\cos(\frac{n\pi x}{w}),
$$

where

$$
\begin{aligned}
f_n(x) &= \left[2(-1)^{n+1} Si(\frac{x(n\pi - wk_0)}{w}) + Si(\frac{(x+w)(n\pi - wk_0)}{w}) \right. \\
&\quad - Si(\frac{(w-x)(n\pi - wk_0)}{w}) + (-1)^{n+1} Si(\frac{(w+x)(n\pi + wk_0)}{w}) \\
&\quad \left. + 2Si(\frac{x(n\pi + wk_0)}{w}) + (-1)^n Si(\frac{(w-x)(n\pi + wk_0)}{w}) \right]. \qquad (4.35)
\end{aligned}
$$

and $R(x)$ is a $O(\frac{n\pi}{w})$ function. As a result,

$$
\begin{aligned}
& [T \circ E_0(\sin(\frac{n\pi x}{w})) - T \circ E_p(\sin(\frac{n\pi x}{w})) + O(\frac{n\pi}{w}) \\
&= -\nu_n \left[1 - \frac{Si(w - n\pi) + Si(w + n\pi)}{2\pi} \right] \sin(\frac{n\pi x}{w}) - \frac{ik_0}{4\pi} f_n(x) \sin(\frac{n\pi x}{w})
\end{aligned}
$$

By comparing (1.7) with (3.14) and using the above estimate, the improved mode matching solution is derived

$$
\tilde{u}(x,y) = \sum_{n=1}^{[w/\pi]-1} \tilde{a}_n \sin(\frac{n\pi x}{w}) \sinh(\gamma_n(y+d)), \qquad (4.36)
$$

where $\tilde{a}_n$ could be obtained from

$$
\begin{aligned}
& \tilde{a}_n \left[\gamma_n \coth(\gamma_n d) - \frac{\nu_n}{2} - \frac{ik_0}{4\pi} f_n(x) \right] \\
&= b_n(\gamma_n \coth(\gamma_n d) - \nu_n). \qquad (4.37)
\end{aligned}
$$

The main result of this work is:

Theorem 1.4.1. *Denote u as the exact solution of (1.7). Then $u \in H_0^{1+\delta}([0,w])$. Let $\tilde{u}$ be defined as (4.36). Then*

$$||u(x,0) - \tilde{u}(x,0)||_2 = O(\frac{1}{w^{1/2}}).$$

Proof. From the lemmas, the coefficients a_n of the exact solution satisfies

$$\begin{aligned} & a_n \left[\gamma_n \coth(\gamma_n d) - \frac{\nu_n}{2} - \frac{ik_0}{4\pi} f_n(x) + O(\frac{n\pi}{w}) \right] \\ = \; & b_n(\gamma_n \coth(\gamma_n d) - \nu_n). \end{aligned}$$

Because $Si(x)$ is bounded, therefore

$$I_1 = \frac{\gamma_n \coth(\gamma_n d) - \nu_n}{\gamma_n \coth(\gamma_n d) - \frac{\nu_n}{2} - \frac{ik_0}{4\pi} f_n(x)} = O(1).$$

Because $a_n = O(b_n)$, from Theorem 1.3.1,

$$||u||_2^2 = \sum_{n=1}^{[w/\pi]-1} (a_n \sinh(\gamma_n d))^2 + O(\frac{1}{w}).$$

For $n\pi < w$,

$$\tilde{a}_n = a_n + O(\frac{n\pi}{w}) b_n$$

Use Theorem 1.3.1 again,

$$||u - \tilde{u}||_2^2 = O(\frac{1}{w})$$

□

Remark 1.4.4. *Consider the following two Helmholtz equations,*

$$\frac{\partial^2 u}{\partial x^2} + \frac{\partial^2 u}{\partial y^2} + k_1^2 u = 0, \quad [0, w] \times [-d, 0].$$

$$\frac{\partial^2 u}{\partial x^2} + \frac{\partial^2 u}{\partial y^2} + k_2^2 u = 0, \quad [0, w] \times [-d, 0]. \tag{4.38}$$

Using the change of variables, (4.38) could be rewritten as

$$\frac{\partial^2 u}{\partial x^2} + \frac{\partial^2 u}{\partial y^2} + k_1^2 u = 0, \quad [0, \frac{k_2}{k_1} w] \times [-\frac{k_2}{k_1} d, 0].$$

Obviously, solving a problem with fixed dimensions at the extremely high frequency is equivalent to solve a problem with the fixed frequency and large d and w. Above the improved mode matching method is derived for large w, which could be viewed as the electrical width of the cavity, i.e., $w_e = w_p/wavelength$. Notice the convergence is not related with depth d. The method should be extremely useful for deep cavity as well.

For a two-layered medium (parallel layer), the modified upper field $\tilde{u}_1$ and the modified lower field $\tilde{u}_2$ are given by

$$\begin{aligned}
\tilde{u}_1(x, y) &= \sum_{n=1}^{\infty} [\tilde{c}_n \sinh(\beta_n(y+d)) + \tilde{d}_n \cosh(\beta_n(y+d))] \sin(\frac{n\pi x}{w}), \\
\tilde{u}_2(x, y) &= \sum_{n=1}^{\infty} \tilde{b}_n \sin(\frac{n\pi x}{w}) \sinh(\gamma_n(y+d)),
\end{aligned}$$

where $\tilde{b}_n$, $\tilde{c}_n$, $\tilde{d}_n$ are solved from the following system,

$$\begin{bmatrix} 0 & A & B \\ -C & D & E \\ -F & G & H \end{bmatrix} \begin{pmatrix} \tilde{b}_n - b_n \\ \tilde{c}_n - c_n \\ \tilde{d}_n - d_n \end{pmatrix} = \begin{pmatrix} R \\ 0 \\ 0 \end{pmatrix}.$$

Here

$$\begin{aligned}
A &= \cosh(\beta_n d)\beta_n - \sinh(\beta_n d)(\nu_n + f_n), & E &= \cosh(\beta_n(d - d_1)), \\
R &= c_n \sinh(\beta_n d) f_n + d_n \cosh(\beta_n d) f_n, & D &= \sinh(\beta_n(d - d_1)), \\
B &= \sinh(\beta_n d)\beta_n - \cosh(\beta_n d)(nu_n + f_n), & C &= \sinh(\gamma_n(d - d_1)), \\
G &= \beta_n \cosh(\beta_n(d - d_1)), & H &= \beta_n \sinh(\beta_n(d - d_1)) \\
F &= \gamma_n \cosh(\beta_n(d - d_1)).
\end{aligned}$$

where β_n, γ_n and ν_n are defined in (3.21), (3.21) and (3.17) respectively. The coefficients of the mode matching solution b_n, c_n, d_n are defined in (3.21), (3.22) and (3.23). The above main theorem is also true for the two-layered cavity case.

If the medium is vertical layered, the error estimate could be obtained by analyzing

$$\int \frac{1}{\sqrt{1-\xi^2}} E_0(\cos(\frac{n\pi x}{w})\hat{)} d\xi.$$

1.5 Numerical Experiments

Here some numerical results for large cavities are presented. It should be noticed that the usual numerical simulations are done for open ended parallel plate waveguide, which has different geometry and different applications. Figure 1.5 displays the magnitude of the aperture field at a high frequency. In this case, $k_0 = 2\pi$, $w = 16$, $d = 4$, $\theta_i = 0$. Here the parameters are already rescaled by the wavelength. Figure 1.6 shows the magnitude of the field of a very wide and shallow cavity. In this case, $k_0 = 2\pi$, $w = 1000/2/\pi$, $d = 0.01/2/\pi$, $\theta_i = 0$. Physically, when $w >> d$, it becomes a total reflection problem, thus $|u| \approx 2\sin(k_0 d)$. The phenomenon may be observed from Figure 1.6. In Figure 1.5 and Figure 1.6, the cavity is empty, i.e., $\epsilon_r = 1$.

Figure 1.7 shows the magnitudes of the fields of a cavity with layered mediums. In this case,

$k_0 = 2\pi$, $w = 50/\pi$, $\theta_i = 0$,

$$\epsilon_r(x) = \begin{cases} 1, & y \in [-5/\pi, 0], \\ \epsilon_2, & y \in [-10/\pi, -5/\pi]. \end{cases}$$

The connected line is for $\epsilon_2 = 1$, the dashed line is for $\epsilon_2 = 3 + 3i$.

Figure 1.8 again shows the magnitudes of the fields of a filled cavity. Here $k_0 = 2\pi$, $w = 8$,

$$\epsilon_r(x) = \begin{cases} \epsilon_1, & y \in [-2.4, 0], \\ \epsilon_2, & y \in [-4.8, -2.4]. \end{cases}$$

The continuous line is for $\epsilon_2 = 1$, the dashed line is for $\epsilon_2 = 4 + i$.

Another important quantity in the EM field calculation is radar cross section (or echo area). It is the most common scattering measurement in antenna design. It

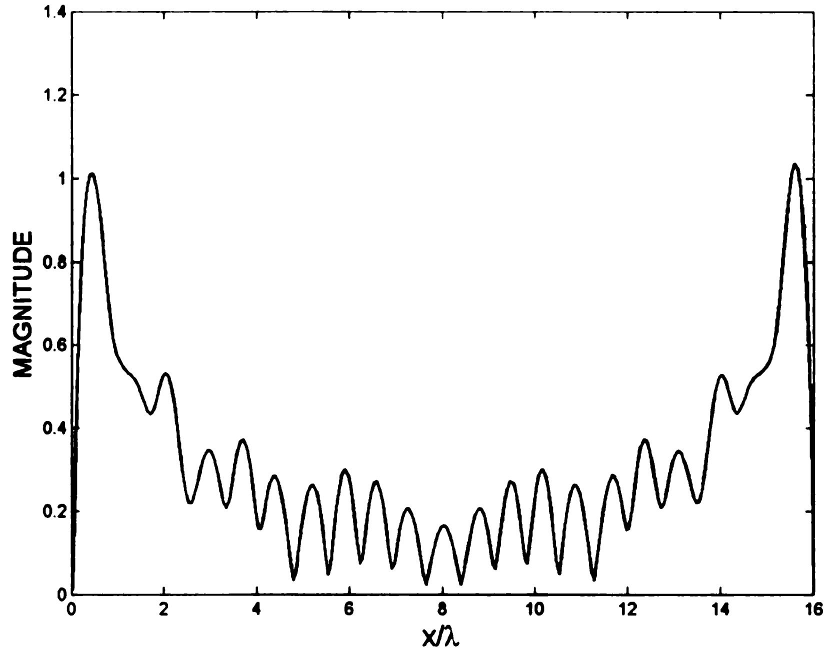

Figure 1.5. Magnitude of the aperture field for a moderately wide cavity.

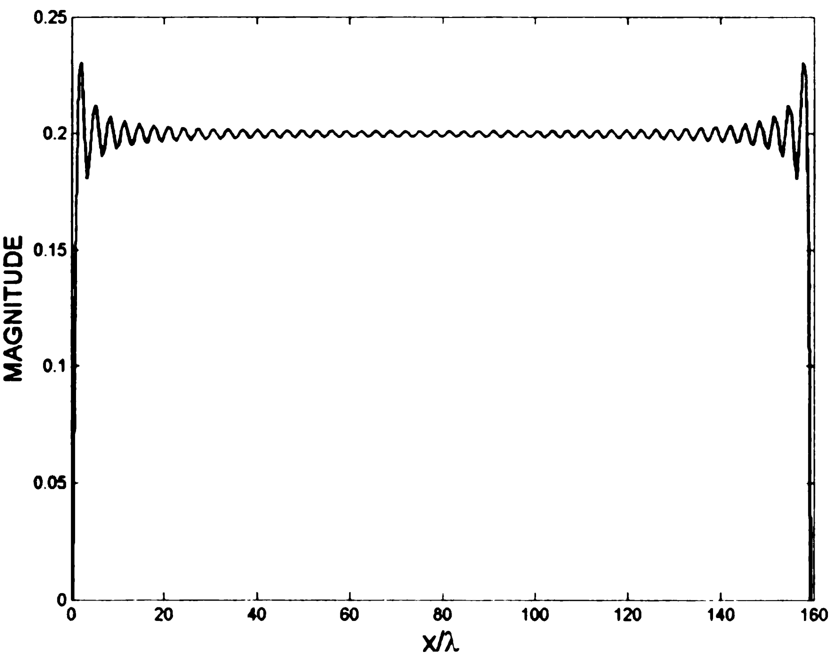

Figure 1.6. Magnitude of the aperture field for a very wide cavity.

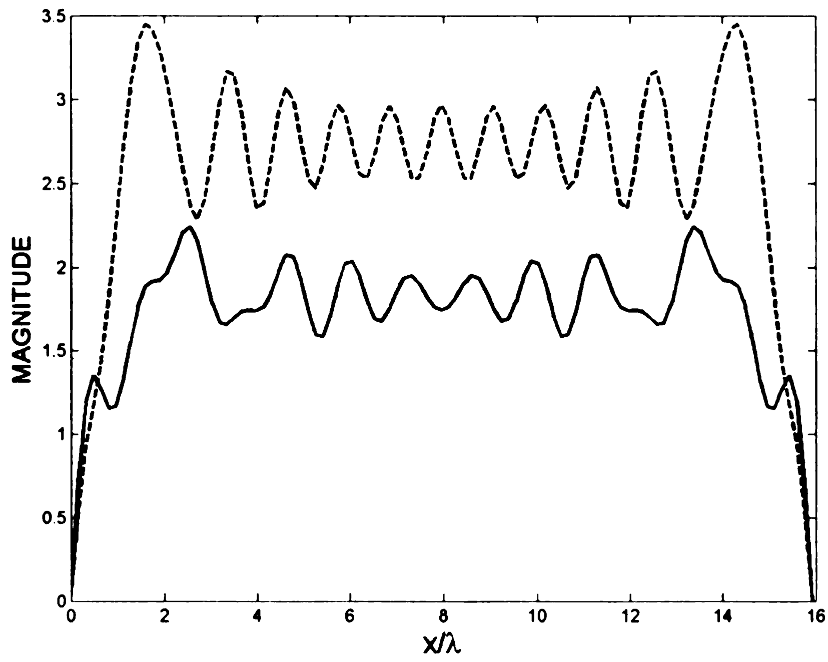

Figure 1.7. Magnitude of the aperture field for a two-layered filled cavity.

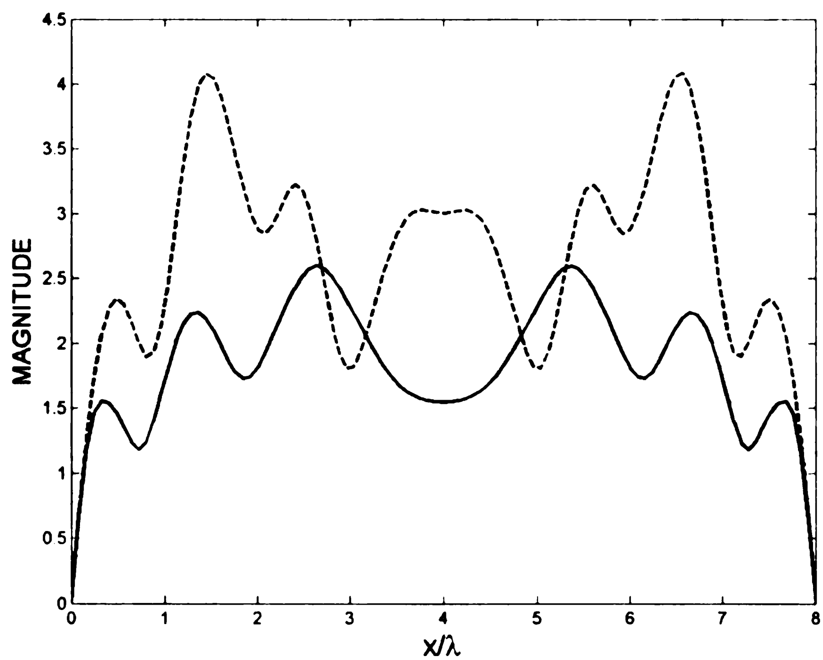

Figure 1.8. Magnitude of the aperture field for a two-layered filled cavity.

measures the "size" of an object as seen at a particular wavelength and polarization and defined by

$$\lim_{r \to \infty} 4\pi r^2 \frac{D_{in}}{D_s}$$

where D_{in} and D_s are incident power density and scattering power density, respectively. The prediction and reduction of Radar Cross section plays an very important role in aircraft design and antenna design.

Mathematically, for the 2-dimensional open cavity, the echo width (Radar Cross Section) is given as [8]

$$\sigma(\phi) \quad = \quad \frac{4}{k} \left| \frac{k}{2} cos(\phi) \int_{\Gamma} e^{i\alpha x} E(x) dx \right|^2 \tag{5.39}$$

Figure 1.9 displays TM case monostatic RCS of a empty cavity with $w = 1$, $d = 0.25$. RCS computed using the FEM (continuous line) and IMM (dashed line) agree well. The unit of RCS is dB/m.

Figure 1.10 shows the monostatic RCS of a filled cavity ($\epsilon_2 = 4 + i$). It follows the same dimension as the previous example. Because of the different choice of time harmonic, the result is compared with the example in [8] for $\epsilon_2 = 4 - i$. IMM result (continuous line) and FEM result are showed in one graph and they agree well with each other.

Figure 1.11 show the RCS of a large cavity. In this case, $w = 10.2$, $d = 5.1$, $\epsilon = 4$ and $f = 300MHz$. The continuous line is for backscattered RCS, the dashed line is for specular RCS.

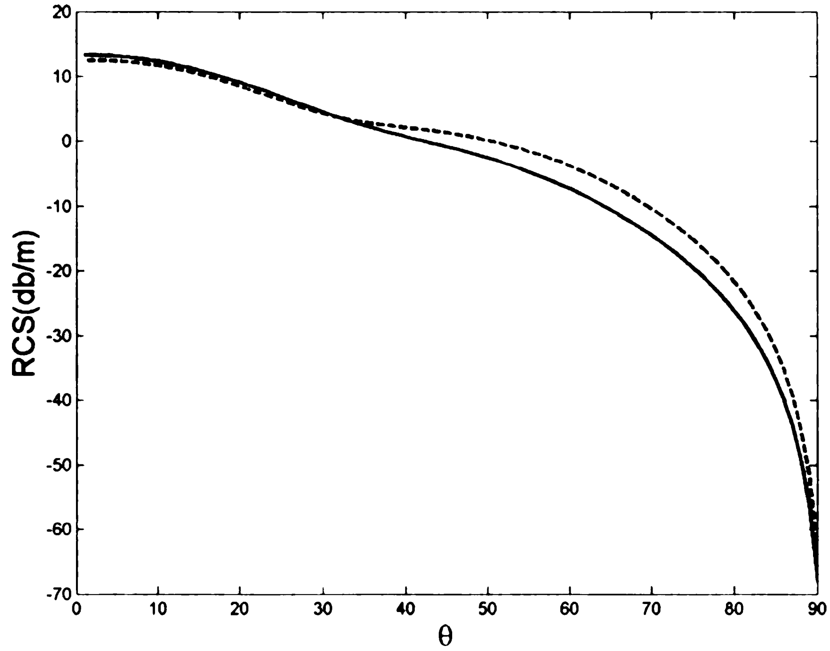

Figure 1.9. RCS of a empty cavity.

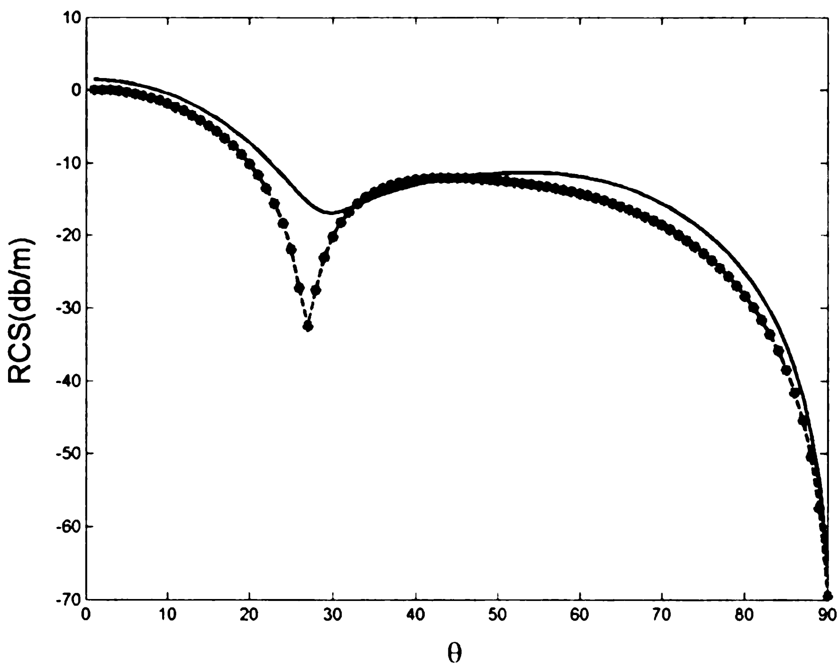

Figure 1.10. Monostatic rcs of a filled cavity.

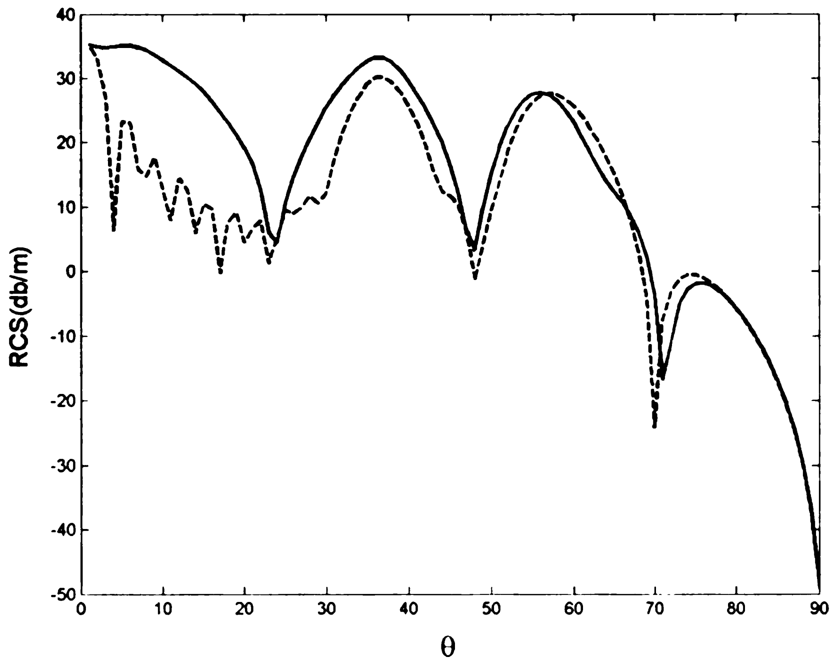

Figure 1.11. Monostatic rcs of a large cavity.

CHAPTER 2

THREE DIMENSIONAL CAVITY PROBLEM

2.1 Formulation

Consider the problem of scattering by a cavity embedded in an infinite ground plane (see Fig 1.1). Assume the ground plane and the cavity walls are perfect electric conductors (PEC). As discussed in Chapter 1, the governing equations are the Maxwell's equations

$$\nabla \times E - i\omega\mu H = 0$$

$$\nabla \times H + i\omega\epsilon E = 0$$

where E and H are the electric and magnetic fields, respectively. Assume k_0 is the wave number and $\hat{x} = (x, y, z)$. Let a plane wave $E^i = Z_0 \hat{p} e^{ik_0 \hat{q}\cdot\hat{x}}$ illuminate on the structure. Here $\hat{p} = \cos\alpha(\sin\phi, -\cos\phi, 0)^T + \sin\alpha(\cos\phi\cos\theta, \sin\phi\cos\theta, \sin\theta)^T$ is the polarization vector, where α is the polarization angle. $\hat{q} = (\cos\phi\sin\theta, \sin\phi\sin\theta, -\cos\theta)^T$ is the wave propagation direction

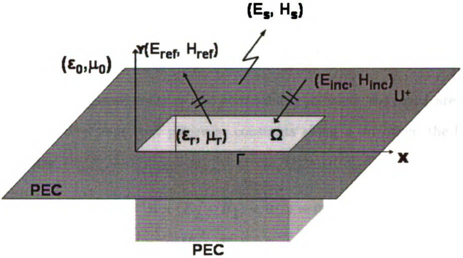

and $Z_0 \approx 120\pi$ is the intrinsic impedance of free space. Then

$$
\begin{aligned}
E^r &= -Z_0 \hat{p^*} e^{ik_0 q^* x} \\
H^i &= \hat{s} e^{ik_0 q x} \\
H^r &= -\hat{s^{**}} e^{ik_0 q^* x}
\end{aligned}
$$

where

$$
p \cdot q = 0 \qquad q^* = (q_1, q_2, -q_3)
$$

$$
s = p \times q \quad s^{**} = (-s_1, -s_2, s3)
$$

Because this is a unbounded scattering problem and can be regarded as a perturbation of total reflection problem, the scattering fields are set as $E^s = E^t - E^i - E^r$ and $H^s = H^t - H^i - H^r$, where E^t and H^t are the total field. In this case the scattering fields satisfy the Silver-Muller radiation condition

$$\lim_{r\to\infty} rE^s = \lim_{r\to\infty} rH^s = 0$$

$$\lim_{r\to\infty} r\{E^s - Z_0 H^s \times r\} = 0$$

Further assume the permittivity ϵ_r and permeability μ_r inside the cavity are invariant along x and y directions, but piecewise constants along z direction, the boundary conditions are

$$n \times (E_1 - E_2) = 0 \quad z = 0$$

$$n \times (H_1 - H_2) = 0 \quad z = 0$$

$$n \cdot (D_1 - D_2) = \rho_s \quad z = 0$$

$$n \cdot (H_1 - H_2) = J_s \quad z = 0$$

where ρ_s and J_s are the surface change density and surface current density.

Notice the cavity walls are PECs, therefore the fields satisfy the following boundary conditions inside the cavity

$$n \times E_2 = 0 \quad \text{on the cavity walls}$$

$$n \cdot H_2 = 0 \quad \text{on the cavity walls}$$

The well-posedness of the variational formulation was discussed in [3] using the Hodge decomposition and the Unique continuation.

2.2 Field Representations

Use PEC conditions, the E field inside the cavity is expanded as

$$E_x = \sum_{m,n=0}^{\infty} \left[\tilde{a}_{mn} \sin(\frac{n\pi x}{w_1}) + a_{mn} \cos(\frac{n\pi x}{w_1})\right] \sin(\frac{m\pi y}{w_2}) \sin[\lambda_{mn}(z+d)], \quad (2.1)$$

$$E_y = \sum_{m,n=0}^{\infty} \sin(\frac{n\pi x}{w_1}) \left[\tilde{b}_{mn} \sin(\frac{m\pi y}{w_2}) + b_{mn} \cos(\frac{m\pi y}{w_2})\right] \sin[\lambda_{mn}(z+d)], \quad (2.2)$$

$$E_z = \sum_{m,n=0}^{\infty} \sin(\frac{n\pi x}{w_1}) \sin(\frac{m\pi y}{w_2}) \{\tilde{c}_{mn} \sin \lambda_{mn}(z+d) + c_{mn} \cos[\lambda_{mn}(z+d)]\} \quad (2.3)$$

where $\lambda_{mn} = \sqrt{k_0^2 \mu_1 \epsilon_1 - (n\pi/w_1)^2 - (m\pi/w_2)^2}$.

Note that $\nabla \cdot \epsilon E = 0$ and the medium is piecewise constant,

$$\begin{aligned}
0 &= \frac{\partial E_x}{\partial x} + \frac{\partial E_y}{\partial y} + \frac{\partial E_z}{\partial z} \\
&= \sum_{m,n=0}^{\infty} \left[\tilde{a}_{mn} \cos(\frac{n\pi x}{w_1}) - a_{mn} \sin(\frac{n\pi x}{w_1})\right] \frac{n\pi}{w_1} \sin(\frac{m\pi y}{w_2}) \sin[\lambda_{mn}(z+d)] \\
&+ \sum_{m,n=0}^{\infty} \sin(\frac{n\pi x}{w_1}) \left[\tilde{b}_{mn} \cos(\frac{m\pi y}{w_2}) - b_{mn} \sin(\frac{m\pi y}{w_2})\right] \frac{m\pi}{w_2} \sin[\lambda_{mn}(z+d)] \\
&+ \sum_{m,n=0}^{\infty} \sin(\frac{n\pi x}{w_1}) \sin(\frac{m\pi y}{w_2}) \{\tilde{c}_{mn} \cos \lambda_{mn}(z+d) - c_{mn} \sin[\lambda_{mn}(z+d)]\} \lambda_{mn}.
\end{aligned}$$

therefore

$$\begin{aligned}
\sum_n \tilde{a}_{mn} n \sin \gamma_{mn}(z+d) &= 0, \\
\sum_m \tilde{b}_{mn} m \sin \gamma_{mn}(z+d) &= 0, \\
\tilde{c}_{mn} \gamma_{mn} &= 0
\end{aligned}$$

Since the coefficient matrix involving $\tilde{a}_{mn}$ is nonsingular, $\tilde{a}_{mn} = 0$, $\tilde{b}_{mn} = 0$, $\tilde{c}_{mn} = 0$ for $\gamma_{mn} \neq 0$ and

$$\frac{n\pi}{w_1} a_{mn} + \frac{m\pi}{w_2} b_{mn} + \lambda_{mn} c_{mn} = 0 \quad (2.4)$$

From the Maxwell's equations, the H field inside the cavity is

$$H_x = \sum_{m,n=0}^{\infty} \frac{1}{i\omega\mu} \left\{ \frac{m\pi}{w_2} c_{mn} \sin(\frac{n\pi x}{w_1}) \cos(\frac{m\pi y}{w_2}) \cos[\lambda_{mn}(z+d)] \right. \tag{2.5}$$

$$\left. -\lambda_{mn} b_{mn} \sin(\frac{n\pi x}{w_1}) \cos(\frac{m\pi y}{w_2}) \cos[\lambda_{mn}(z+d)] \right\},$$

$$H_y = \sum_{m,n=0}^{\infty} \frac{1}{i\omega\mu} \left\{ \lambda_{mn} a_{mn} \cos(\frac{n\pi x}{w_1}) \sin(\frac{m\pi y}{w_2}) \cos[\lambda_{mn}(z+d)] \right. \tag{2.6}$$

$$\left. - \frac{n\pi}{w_1} c_{mn} \cos(\frac{n\pi x}{w_1}) \sin(\frac{m\pi y}{w_2}) \cos[\lambda_{mn}(z+d)] \right\},$$

$$H_z = \sum_{m,n=0}^{\infty} \frac{1}{i\omega\mu} \left\{ \frac{n\pi}{w_1} b_{mn} \cos(\frac{n\pi y}{w_1}) \cos(\frac{m\pi x}{w_2}) \sin[\lambda_{mn}(z+d)] \right. \tag{2.7}$$

$$\left. - \frac{m\pi}{w_2} a_{mn} \cos(\frac{n\pi x}{w_1}) \cos(\frac{m\pi y}{w_2}) \sin[\lambda_{mn}(z+d)] \right\}.$$

Next, the field representations in the region of upper half plan are established .

Above the ground, ϵ_0 and μ_0 are constants everywhere. Thus from the Maxwell's equations,

$$\begin{cases} \Delta E_{x,y} + k_0^2 E_{x,y} = 0 & \text{when } z > 0 \\ E_{x,y} = 0 & \text{when } z = 0. \end{cases}$$

and the scattering components $E^s_{x,y}$ satisfy the Maxwell's equations and the Silver Muller radiation condition. Further more,

$$E^s_{x,y}(x, y, 0) = E_{x,y}(x, y, 0).$$

Take the Fourier transform with respect to x and y of the Maxwell's equations and solve an ODE for z [2]. In this case, the x y scattering components of the E field above the ground is derived as

$$\hat{E}^s(\xi, z) = \hat{E}^s(\xi, 0) e^{i\sqrt{k_0^2 - \xi_1^2 - \xi_2^2}\, z}, \tag{2.8}$$

$$E^s_{x,y}(x, y, z) = \frac{1}{2\pi} \int_{-\infty}^{\infty} (E_0 \circ E_{x,y})\hat{}(\xi, 0) e^{i\sqrt{k_0^2 - \xi_1^2 - \xi_2^2}\, z} e^{i\xi_1 x + i\xi_2 y} d\xi. \tag{2.9}$$

Note that give $E_z^s(x,y,0) \neq E_z(x,y,0)$, a similar result could not be derived for E_z.

For E_z,

$$\hat{E}_z^s(\xi_1,\xi_2,z) = [E_0(E_z^s(\xi_1,\xi_2,0))]\hat{}\, e^{i\sqrt{k_0^2-\xi_1^2-\xi_2^2}z}$$

Hence,

$$\partial_z \hat{E}_z^s(\xi_1,\xi_2,z) = i\sqrt{k_0^2-\xi_1^2-\xi_2^2}\,[E_0(E_z^s(\xi_1,\xi_2,0))]\hat{}\, e^{i\sqrt{k_0^2-\xi_1^2-\xi_2^2}z}$$

Therefore

$$[E_0(E_z^s(\xi_1,\xi_2,0))]\hat{}\, e^{i\sqrt{k_0^2-\xi_1^2-\xi_2^2}z} = \partial_z \hat{E}_z^s(\xi_1,\xi_2,z)\frac{1}{i\sqrt{k_0^2-\xi_1^2-\xi_2^2}}$$

it implies

$$\hat{E}_z^s(\xi_1,\xi_2,z) = \partial_z \hat{E}_z^s(\xi_1,\xi_2,z)\frac{1}{i\sqrt{k_0^2-\xi_1^2-\xi_2^2}}$$

Taking the derivative of $\hat{E}_z^s$ with respect to z and using $\nabla\cdot\epsilon E = 0$ [2], [22],

$$\hat{E}_z^s(\xi,z) = [-(\partial_x E_x^s)\hat{}(\xi,z) - (\partial_y E_y^s)\hat{}(\xi,z)]\frac{1}{i\sqrt{k_0^2-\xi_1^2-\xi_2^2}}$$

$$\begin{aligned} & E_z^s(x,y,z) \\ = \;& \frac{1}{2\pi}\int_{R^2}[-(\partial_x E_x^s)\hat{}(\xi,z) - (\partial_y E_y^s)\hat{}(\xi,z)]\frac{1}{i\sqrt{k_0^2-\xi_1^2-\xi_2^2}}e^{i\xi_1 x + i\xi_2 y}d\xi \end{aligned}$$

for $z \geq 0$. From the radiation condition $|E| = O(1/r)$, $(\partial_x E_x^s)\hat{} = i\xi_1 \hat{E}_x^s$. Thus the total E field above the ground is

$$\begin{aligned} & E_{x,y}(x,y,z) && (2.10) \\ = \;& Z_0 p_{1,2} e^{i(k_x x + k_y y)}(-e^{ik_z z} + e^{-ik_z z}) \\ + \;& \frac{1}{2\pi}\int_{-\infty}^{\infty}(E_0 \circ E_{x,y})\hat{}(\xi,0)e^{i\sqrt{k_0^2-\xi_1^2-\xi_2^2}z}e^{i\xi_1 x + i\xi_2 y}d\xi. && (2.11) \end{aligned}$$

$$
\begin{aligned}
& E_z(x,y,z) && (2.12)\\
= \ & Z_0 p_3 e^{i(k_x x+k_y y)}(e^{ik_z z}+e^{-ik_z z}) && (2.13)\\
+ \ & \frac{1}{2\pi}\int_{R^2}[-\xi_1 \hat{E}_x^s(\xi,z)-\xi_2 \hat{E}_y^s(\xi,z)]\frac{1}{\sqrt{k_0^2-\xi_1^2-\xi_2^2}}e^{i\xi_1 x+i\xi_2 y}d\xi
\end{aligned}
$$

where $\xi = (\xi_1, \xi_2)$.

From the Maxwell's equations, the x-y components of the magnetic field above the ground are

$$
\begin{aligned}
& H_x(x,y,0) && (2.14)\\
= \ & \frac{1}{i\omega\mu}\Big\{2Z_0 i(k_y p_3 + k_z p_2)e^{i(k_x x+k_y y)} && (2.15)\\
+ \ & \frac{1}{2\pi}\int_{R^2}[-\xi_1(E_0\circ E_x)\hat{}(\xi,0)-\xi_2(E_0\circ E_y)\hat{}(\xi,0)]\frac{i\xi_2 e^{i\xi_1 x+i\xi_2 y}}{\sqrt{k_0^2-\xi_1^2-\xi_2^2}}d\xi\\
- \ & \frac{1}{2\pi}\int_{R^2} i\sqrt{k_0^2-\xi_1^2-\xi_2^2}\,(E_0\circ E_y)\hat{}(\xi,0)e^{i\xi_1 x+i\xi_2 y}d\xi\ \Big\}
\end{aligned}
$$

$$
\begin{aligned}
& H_y(x,y,0) && (2.16)\\
= \ & \frac{1}{i\omega\mu}\Big\{2Z_0 i(-k_z p_1 - k_x p_3)e^{i(k_x x+k_y y)} && (2.17)\\
- \ & \frac{1}{2\pi}\int_{R^2}[-\xi_1(E_0\circ E_x)\hat{}(\xi,0)-\xi_2(E_0\circ E_y)\hat{}(\xi,0)]\frac{i\xi_1 e^{i\xi_1 x+i\xi_2 y}}{\sqrt{k_0^2-\xi_1^2-\xi_2^2}}d\xi\\
+ \ & \frac{1}{2\pi}\int_{R^2} i\sqrt{k_0^2-\xi_1^2-\xi_2^2}\,(E_0\circ E_x)\hat{}(\xi,0)e^{i\xi_1 x+i\xi_2 y}d\xi\ \Big\}
\end{aligned}
$$

From the continuity conditions and application of (2.1) to the above equations, two equations involving a_n, b_n, c_n are derived. Combining with (2.4), the electromagnetic fields could be solved.

2.3 Mode Matching Method

Replacing the zero extension E_0 in (2.14), (2.16) by the periodic extension E_P,

$$
\begin{aligned}
& H_x(x,y,0) && (3.18)\\
= & \frac{1}{i\omega\mu}\{\, 2Z_0 i(k_y p_3 + k_z p_2)e^{i(k_x x+k_y y)} && (3.19)\\
& +\frac{1}{2\pi}\int_{R^2}[-\xi_1(E_P\circ E_x)\hat{}(\xi,0)-\xi_2(E_P\circ E_y)\hat{}(\xi,0)]\frac{i\xi_2 e^{i\xi_1 x+i\xi_2 y}}{\sqrt{k_0^2-\xi_1^2-\xi_2^2}}d\xi\\
& -\frac{1}{2\pi}\int_{R^2} i\sqrt{k_0^2-\xi_1^2-\xi_2^2}\,(E_P\circ E_y)\hat{}(\xi,0)e^{i\xi_1 x+i\xi_2 y}d\xi\,\}
\end{aligned}
$$

$$
\begin{aligned}
& H_y(x,y,0) && (3.20)\\
= & \frac{1}{i\omega\mu}\{\, 2Z_0 i(-k_z p_1 - k_x p_3)e^{i(k_x x+k_y y)} && (3.21)\\
& -\frac{1}{2\pi}\int_{R^2}[-\xi_1(E_P\circ E_x)\hat{}(\xi,0)-\xi_2(E_P\circ E_y)\hat{}(\xi,0)]\frac{i\xi_1 e^{i\xi_1 x+i\xi_2 y}}{\sqrt{k_0^2-\xi_1^2-\xi_2^2}}d\xi\\
& +\frac{1}{2\pi}\int_{R^2} i\sqrt{k_0^2-\xi_1^2-\xi_2^2}\,(E_P\circ E_x)\hat{}(\xi,0)e^{i\xi_1 x+i\xi_2 y}d\xi\,\}
\end{aligned}
$$

It is easy to derive

$$
\begin{aligned}
(E_P\cos(\frac{n\pi}{w}\cdot))\hat{}\,(\xi) &= \frac{\pi}{\sqrt{2\pi}}(\delta(\xi+\frac{n\pi}{w})+\delta(\xi-\frac{n\pi}{w})),\\
(E_0\cos(\frac{n\pi}{w}\cdot))\hat{}\,(\xi) &= \frac{1}{\sqrt{2\pi}}(-i\xi)\left(\frac{1-(-1)^n e^{-iw\xi}}{\xi^2-(\frac{n\pi}{w})^2}\right),
\end{aligned}
$$

where $\delta(\cdot)$ is the Dirac delta function.

Lemma 2.3.1. *For the periodic extension E_P, the following statements are hold:*

$$
\begin{aligned}
& \frac{1}{2\pi}\int_{R^2}[E_P(\sin\frac{n\pi x}{w_1}\cos\frac{m\pi y}{w_2})]\hat{}\sqrt{k_0^2-\xi_1^2-\xi_2^2}e^{i(x\xi_1+y\xi_2)}d\xi\\
= & \lambda_{mn}\sin\frac{n\pi x}{w_1}\cos\frac{m\pi y}{w_2}\\
& \frac{1}{2\pi}\int_{R^2}[E_P(\cos\frac{n\pi x}{w_1}\sin\frac{m\pi y}{w_2})]\hat{}\sqrt{k_0^2-\xi_1^2-\xi_2^2}e^{i(x\xi_1+y\xi_2)}d\xi\\
= & \lambda_{mn}\cos\frac{n\pi x}{w_1}\sin\frac{m\pi y}{w_2}
\end{aligned}
$$

Lemma 2.3.2. *For the periodic extension E_p, the following statements are hold:*

$$\frac{1}{2\pi}\int_{R^2}[E_p(\cos\frac{n\pi x}{w_1}\sin\frac{m\pi y}{w_2})]^{\wedge}\frac{\xi_1^2 e^{i(x\xi_1+y\xi_2)}}{\sqrt{k_0^2-\xi_1^2-\xi_2^2}}d\xi = \frac{(\frac{n\pi}{w_1})^2}{\lambda_{mn}}\cos\frac{n\pi x}{w_1}\sin\frac{m\pi y}{w_2}$$

$$\frac{1}{2\pi}\int_{R^2}[E_p(\sin\frac{n\pi x}{w_1}\cos\frac{m\pi y}{w_2})]^{\wedge}\frac{\xi_1\xi_2 e^{i(x\xi_1+y\xi_2)}}{\sqrt{k_0^2-\xi_1^2-\xi_2^2}}d\xi = \frac{\frac{nm\pi^2}{w_1w_2}}{\lambda_{mn}}\cos\frac{n\pi x}{w_1}\sin\frac{m\pi y}{w_2}$$

$$\frac{1}{2\pi}\int_{R^2}[E_p(\sin\frac{n\pi x}{w_1}\cos\frac{m\pi y}{w_2})]^{\wedge}\frac{\xi_2^2 e^{i(x\xi_1+y\xi_2)}}{\sqrt{k_0^2-\xi_1^2-\xi_2^2}}d\xi = \frac{(\frac{m\pi}{w_2})}{\lambda_{mn}^2}\sin\frac{n\pi x}{w_1}\cos\frac{m\pi y}{w_2}$$

$$\frac{1}{2\pi}\int_{R^2}[E_p(\cos\frac{n\pi x}{w_1}\sin\frac{m\pi y}{w_2})]^{\wedge}\frac{\xi_1\xi_2 e^{i(x\xi_1+y\xi_2)}}{\sqrt{k_0^2-\xi_1^2-\xi_2^2}}d\xi = \frac{\frac{mn\pi^2}{w_1w_2}}{\lambda_{mn}}\sin\frac{n\pi x}{w_1}\cos\frac{m\pi y}{w_2}$$

Using the continuity conditions

$$H^s_{x,y}(x,y,0^+) + H^i_{x,y}(x,y,0^+) + H^r_{x,y}(x,y,0^+) = H_{x,y}(x,y,0^-)$$

a system equations is derived

$$\frac{1}{\mu_1}[\frac{m\pi}{w_2}c_{mn}\cos(\lambda_{mn}d) - \lambda_{mn}b_{mn}\cos(\lambda_{mn}d)] \tag{3.22}$$

$$= \frac{1}{\mu_0}[S^1_{mn} - a_{mn}i\frac{mn\pi^2}{w_1w_2\lambda_{mn}}\sin(\gamma_{mn}d) - b_{mn}i\frac{m^2\pi^2}{w_2^2\lambda_{mn}}\sin(\gamma_{mn}d) \tag{3.23}$$
$$-i\lambda_{mn}b_{mn}\sin(\lambda_{mn}d)]$$

$$\frac{1}{\mu_1}[\lambda_{mn}a_{mn}\cos(\lambda_{mn}d) - \frac{n\pi}{w_1}c_{mn}\cos(\lambda_{mn}d)] \tag{3.24}$$

$$= \frac{1}{\mu_0}[S^2_{mn} + a_{mn}i\frac{n^2\pi^2}{w_1^2\lambda_{mn}}\sin(\gamma_{mn}d) + b_{mn}i\frac{mn\pi^2}{w_1w_2\lambda_{mn}}\sin(\gamma_{mn}d) \tag{3.25}$$
$$+i\lambda_{mn}a_{mn}\sin(\lambda_{mn}d)]$$

Here

$$\begin{aligned}
S^1_{mn} &= \frac{4}{w_1 w_2}\int_0^{w_2}\int_0^{w_1} e^{ik_x x + k_y y}\sin(\frac{n\pi}{w_1}x)\cos(\frac{m\pi}{w_2}y)dxdy \\
&= \frac{4}{w_1 w_2} B_n(w_1, k_x) A_m(w_2, k_y) \\
S^2_{mn} &= \frac{4}{w_1 w_2}\int_0^{w_2}\int_0^{w_1} e^{ik_x x + k_y y}\cos(\frac{n\pi}{w_1}x)\sin(\frac{m\pi}{w_2}y)dxdy \\
&= \frac{4}{w_1 w_2} B_m(w_2, k_y) A_n(w_1, k_x)
\end{aligned}$$

where

$$A_m(w,k) = \begin{cases} w, & m = 0 \text{ and } k = 0, \\ \dfrac{e^{ikw} - 1}{ik}, & m = 0 \text{ and } k \neq 0, \\ \dfrac{w}{m\pi}\sin(m\pi), & m \neq 0 \text{ and } k = 0, \\ -ik\dfrac{(-1)^m e^{ikw} - 1}{k^2 - (\frac{m\pi}{w})^2}, & m \neq 0 \text{ and } k \neq 0 \end{cases}$$

and

$$B_m(w,k) = \begin{cases} 0, & m = 0, \\ \dfrac{w}{m\pi}(1 - (-1)^m), & m \neq 0 \text{ and } k = 0, \\ \dfrac{m\pi}{w}\dfrac{(-1)^m e^{ikw} - 1}{k^2 - (\frac{m\pi}{w})^2}, & m \neq 0 \text{ and } k \neq 0 \end{cases}$$

Solving (3.22), (3.24) and (2.4), the approximation of the electromagnetic field on the aperture is obtained. Analogous to the two dimensional case, it is called mode matching method.

2.4 Numerical Experiments

For convenience of the later use, here the far zone scattering and radar cross section (RCS) are discussed first.

From (2.9), the field representation above the ground is

$$E^s(r,\theta,\phi) = \frac{1}{2\pi}\int_{-\infty}^{\infty}(E_0 \circ E)\hat{}(\xi, 0)e^{ik\cdot r}d\xi,$$

where $k \cdot r = \sqrt{k_0^2 - \xi_1^2 - \xi_2^2} r \cos\theta + \xi_1 r \sin\theta \cos\phi + i\xi_2 r \sin\theta \sin\phi$ and r, θ and ϕ are the variables in spherical coordinates. Solving

$$\frac{\partial k \cdot r}{\partial \xi_1} = 0, \qquad \frac{\partial k \cdot r}{\partial \xi_2} = 0,$$

the stationary phase point is derived as [22]

$$\xi_1 = k_0 \cos\phi \sin\theta,$$

$$\xi_2 = k_0 \sin\phi \sin\theta.$$

Therefore the far zone scattered field can be computed by

$$E^s(r,\theta,\phi) \approx (E_0 \circ E)\hat{}(k_0 \cos\phi \sin\theta, k_0 \sin\phi \sin\theta, 0) i \frac{e^{ik_0 r}}{r} k_0 \cos\theta,$$

In [8], 3d RCS is defined by

$$\sigma(\theta,\phi,\theta^{inc},\phi^{inc}) = \lim_{r\to\infty} 4\pi r^2 \frac{|E^s(r,\theta,\phi)|^2}{|E^{inc}(\theta^{inc},\phi^{inc})|^2}$$

where θ, ϕ are the observed angles and θ^{inc}, ϕ^{inc} are the incident angles. When incident angles and observed angles are same, σ is monostatic or backscatter radar cross section. Otherwise, it is called bistatic radar cross section.

To incorporate the polarization information, the radar cross section can also be defined as

$$\sigma_{pq}(\theta,\phi,\theta^{inc},\phi^{inc}) = \lim_{r\to\infty} 4\pi r^2 \frac{|E_p^s(r,\theta,\phi)|^2}{|E_q^{inc}(\theta^{inc},\phi^{inc})|^2}$$

or people sometimes use

$$\sigma_{HH} = \lim_{r\to\infty} 4\pi r^2 \frac{|E_\phi^s|^2}{|E_\phi^{inc}|^2}$$

$$\sigma_{HE} = \lim_{r\to\infty} 4\pi r^2 \frac{|E_\theta^s|^2}{|E_\phi^{inc}|^2}$$

$$\sigma_{EE} = \lim_{r\to\infty} 4\pi r^2 \frac{|E_\theta^s|^2}{|E_\theta^{inc}|^2}$$

$$\sigma_{EH} = \lim_{r\to\infty} 4\pi r^2 \frac{|E_\phi^s|^2}{|E_\theta^{inc}|^2}$$

With the far field patter derived above, the RCS is given by

$$
\begin{aligned}
RCS &= \lim_{r\to\infty} 4\pi r^2 \frac{|E^{sc}|^2}{|E^{in}|^2} \\
&= \frac{k_0^2\cos^2\theta}{\pi} \left| \int_0^{w_1}\int_0^{w_2} E(x,y,0) e^{ik_0\sin\theta(x\cos\phi+y\sin\phi)} dxdy \right|^2
\end{aligned}
$$

Let

$$
RCS = (\sum_{m,n} s_x, \sum_{m,n} s_y, \sum_{m,n} s_z),
$$

applying the field representation (2.1), then

- $n = 0, m = 0$

  $s_x = 0, s_y = 0, s_z = 0;$

- $n = 0, m \neq 0$

  $s_x = a_{mn}\sin(\lambda_{mn}d)(-i)\dfrac{m\pi}{w_2} \times P_1 Q_2,$

  $s_y = 0, s_z = 0;$

- $n \neq 0, m = 0$

  $s_y = b_{mn}\sin(\lambda_{mn}d)(-i)\dfrac{n\pi}{w_1} \times P_2 Q_1,$

  $s_x = 0, s_z = 0;$

- $n \neq 0, m \neq 0$

$$
\begin{aligned}
s_x &= a_{mn}\sin(\lambda_{mn}d)(-i)k_0\sin\theta\cos\phi\frac{m\pi}{w_2} \times Q_1Q_2, \\
s_y &= b_{mn}\sin(\lambda_{mn}d)(-i)k_0\sin\theta\sin\phi\frac{n\pi}{w_1} \times Q_1Q_2, \\
s_z &= -\frac{(a_{mn}\frac{n\pi}{w_1} + b_{mn}\frac{m\pi}{w_2})}{\lambda_{mn}}\cos(\lambda_{mn}d)\frac{n\pi}{w_1}\frac{m\pi}{w_2} \times Q_1Q_2.
\end{aligned}
$$

where

$$P_1 = \begin{cases} \dfrac{e^{ik_0 \sin\theta \cos\phi w_1} - 1}{(k_0 \sin\theta \cos\phi)} & \text{if } (k_0 \sin\theta\cos\phi) \neq 0 \\ iw_1 & \text{if } (k_0 \sin\theta\cos\phi) = 0 \end{cases}$$

$$P_2 = \begin{cases} \dfrac{e^{ik_0 \sin\theta \sin\phi w_2} - 1}{(k_0 \sin\theta \sin\phi)} & \text{if } (k_0 \sin\theta\sin\phi) \neq 0 \\ iw_2 & \text{if } (k_0 \sin\theta\sin\phi) = 0 \end{cases}$$

$$Q_1 = \begin{cases} \dfrac{e^{ik_0 \sin\theta \cos\phi w_1}(-1)^n - 1}{(k_0 \sin\theta \cos\phi)^2 - (n\pi/w_1)^2} & \text{if } (k_0 \sin\theta\cos\phi)^2 \neq (n\pi/w_1)^2 \\ \dfrac{iw_1^2}{2n\pi} & \text{if } (k_0 \sin\theta\cos\phi)^2 = (n\pi/w_1)^2 \end{cases}$$

$$Q_2 = \begin{cases} \dfrac{e^{ik_0 \sin\theta \sin\phi w_2}(-1)^m - 1}{(k_0 \sin\theta \sin\phi)^2 - (m\pi/w_2)^2} & \text{if } (k_0 \sin\theta\sin\phi)^2 \neq (m\pi/w_2)^2 \\ \dfrac{iw_2^2}{2m\pi} & \text{if } (k_0 \sin\theta\sin\phi)^2 = (m\pi/w_2)^2 \end{cases}$$

Figure 2.1 and 2.2 show the RCS for a long and narrow cavity ($w_1 = 2.5$, $w_2 = 0.25$, $d = 0.25$). The unit of RCS is dB/m^2. Figure 2.1 presents the back scattering RCS for $\theta = 90^o$. The upper curve is for H polarization and the lower cure is for E polarization. Figure 2.2 presents the back scattering RCS for $\theta = 0^o$. The continuous curve is for H polarization and the dashed curve is for E polarization. They agrees well with the results in [21].

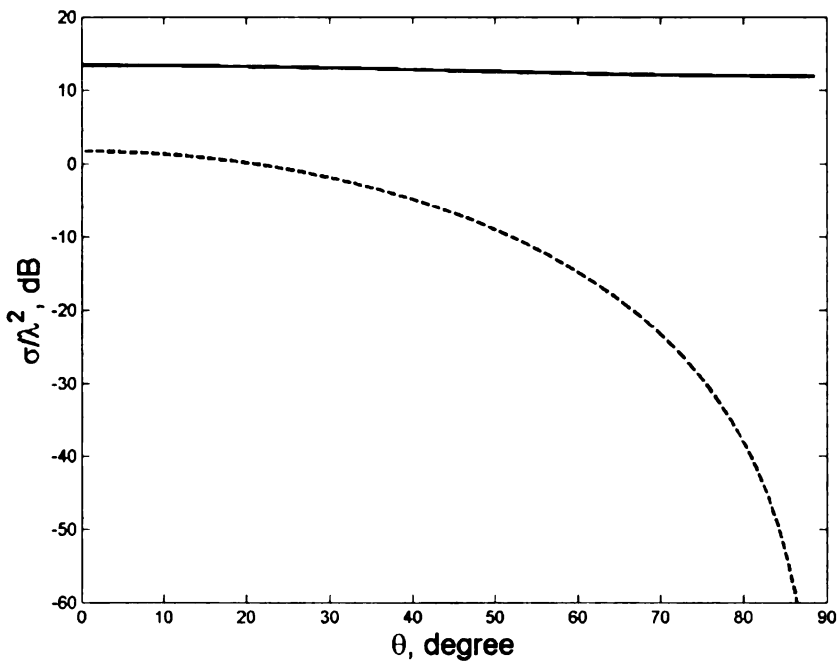

Figure 2.1. Mode matching method ($\phi = 0$).

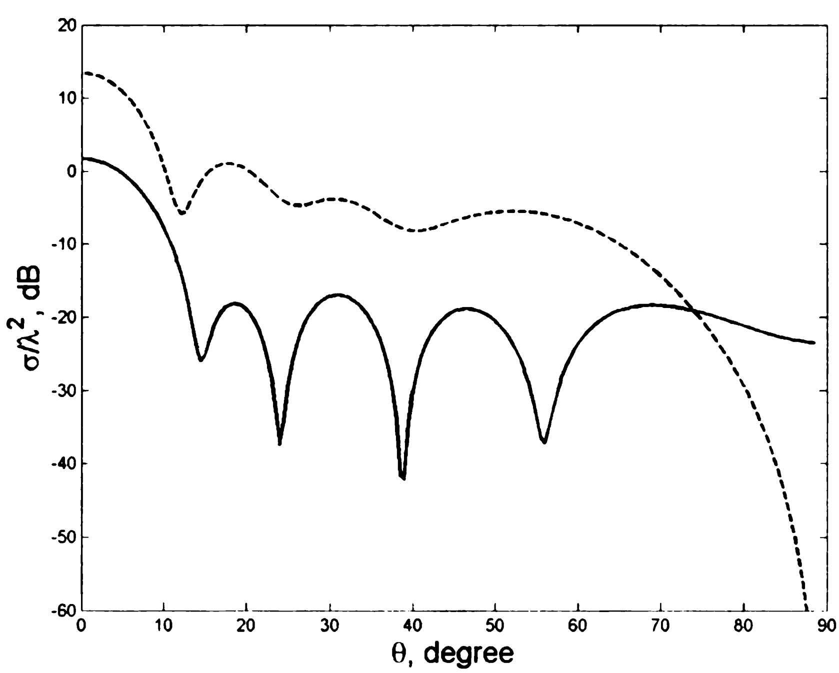

Figure 2.2. Mode matching method ($\phi=\pi/2$).

2.5 Improved Mode Matching Method

From (2.14), (2.16) and after some simple manipulations,

$$
\begin{aligned}
& H_x(x, y, 0) && (5.26)\\
= \; & \frac{1}{i\omega\mu}\{\, 2Z_0 i(k_y p_3 + k_z p_2) e^{i(k_x x + k_y y)} && (5.27)\\
& + \frac{1}{2\pi}\int_{R^2} [-\xi_1 (E_0 \circ E_x)\hat{}(\xi, 0) - \xi_2 (E_0 \circ E_y)\hat{}(\xi, 0)] \frac{i\xi_2 e^{i\xi_1 x + i\xi_2 y}}{\sqrt{k_0^2 - \xi_1^2 - \xi_2^2}} d\xi \\
& - \frac{1}{2\pi}\int_{R^2} i \frac{k_0^2 - \xi_1^2 - \xi_2^2}{\sqrt{k_0^2 - \xi_1^2 - \xi_2^2}} (E_0 \circ E_y)\hat{}(\xi, 0) e^{i\xi_1 x + i\xi_2 y} d\xi \,\}
\end{aligned}
$$

$$
\begin{aligned}
& H_y(x, y, 0) && (5.28)\\
= \; & \frac{1}{i\omega\mu}\{\, 2Z_0 i(-k_z p_1 - k_x p_3) e^{i(k_x x + k_y y)} && (5.29)\\
& - \frac{1}{2\pi}\int_{R^2} [-\xi_1 (E_0 \circ E_x)\hat{}(\xi, 0) - \xi_2 (E_0 \circ E_y)\hat{}(\xi, 0)] \frac{i\xi_1 e^{i\xi_1 x + i\xi_2 y}}{\sqrt{k_0^2 - \xi_1^2 - \xi_2^2}} d\xi \\
& + \frac{1}{2\pi}\int_{R^2} i \frac{k_0^2 - \xi_1^2 - \xi_2^2}{\sqrt{k_0^2 - \xi_1^2 - \xi_2^2}} (E_0 \circ E_x)\hat{}(\xi, 0) e^{i\xi_1 x + i\xi_2 y} d\xi \,\}
\end{aligned}
$$

Lemma 2.5.1. *For the zero extension E_0, the following statements are hold*

$$\int_{R^2}[E_0(\cos\frac{n\pi x}{w_1}\sin\frac{m\pi y}{w_2})]^{\wedge}\frac{\xi_1^2 e^{i(x\xi_1+y\xi_2)}}{\sqrt{k_0^2-\xi_1^2-\xi_2^2}}d\xi$$
$$= (\frac{n\pi}{w_1})^2\int_{R^2}[E_0(\cos\frac{n\pi x}{w_1}\sin\frac{m\pi y}{w_2})]^{\wedge}\frac{e^{i(x\xi_1+y\xi_2)}}{\sqrt{k_0^2-\xi_1^2-\xi_2^2}}d\xi$$

$$\int_{R^2}[E_0(\sin\frac{n\pi x}{w_1}\cos\frac{m\pi y}{w_2})]^{\wedge}\frac{\xi_1\xi_2 e^{i(x\xi_1+y\xi_2)}}{\sqrt{k_0^2-\xi_1^2-\xi_2^2}}d\xi$$
$$= \frac{nm\pi^2}{w_1w_2}\int_{R^2}[E_0(\cos\frac{n\pi x}{w_1}\sin\frac{m\pi y}{w_2})]^{\wedge}\frac{e^{i(x\xi_1+y\xi_2)}}{\sqrt{k_0^2-\xi_1^2-\xi_2^2}}d\xi$$

$$\int_{R^2}[E_0(\sin\frac{n\pi x}{w_1}\cos\frac{m\pi y}{w_2})]^{\wedge}\frac{\xi_2^2 e^{i(x\xi_1+y\xi_2)}}{\sqrt{k_0^2-\xi_1^2-\xi_2^2}}d\xi$$
$$= (\frac{m\pi}{w_2})^2\int_{R^2}[E_0(\sin\frac{n\pi x}{w_1}\cos\frac{m\pi y}{w_2})]^{\wedge}\frac{e^{i(x\xi_1+y\xi_2)}}{\sqrt{k_0^2-\xi_1^2-\xi_2^2}}d\xi$$

$$\int_{R^2}[E_0(\cos\frac{n\pi x}{w_1}\sin\frac{m\pi y}{w_2})]^{\wedge}\frac{\xi_1\xi_2 e^{i(x\xi_1+y\xi_2)}}{\sqrt{k_0^2-\xi_1^2-\xi_2^2}}d\xi$$
$$= \frac{nm\pi^2}{w_1w_2}\int_{R^2}[E_0(\sin\frac{n\pi x}{w_1}\cos\frac{m\pi y}{w_2})]^{\wedge}\frac{e^{i(x\xi_1+y\xi_2)}}{\sqrt{k_0^2-\xi_1^2-\xi_2^2}}d\xi$$

Similar results could be derived if replace the kernel $\frac{1}{\sqrt{k_0^2-\xi_1^2-\xi_2^2}}$ by $\frac{1}{\overline{\sqrt{k_0^2-\xi_1^2-\xi_2^2}}}$, while the second kernel is the conjugate of the first one. Therefore from Lemma 2.5.1, (5.26) and (5.28) become

$$H_x(x,y,0) = \frac{1}{i\omega\mu}\{\, 2Z_0 i(k_y p_3 + k_z p_2)e^{i(k_x x+k_y y)} - \frac{1}{2\pi}\int_{R^2} i\frac{k_0^2}{\overline{\sqrt{k_0^2-\xi_1^2-\xi_2^2}}}(E_0\circ E_y)^{\wedge}(\xi,0)e^{i\xi_1 x+i\xi_2 y}d\xi\,\} + R_2 \tag{5.30}$$

$$
\begin{aligned}
H_y(x,y,0) &= \frac{1}{i\omega\mu}\{\, 2Z_0 i(-k_z p_1 - k_x p_3)e^{i(k_x x+k_y y)} \qquad (5.31)\\
&+\frac{1}{2\pi}\int_{R^2} i\frac{k_0^2}{\sqrt{k_0^2-\xi_1^2-\xi_2^2}}(E_0\circ E_x)\hat{}(\xi,0)e^{i\xi_1 x+i\xi_2 y}d\xi\,\} + R_2
\end{aligned}
$$

Here R_2 takes one of the following forms: $O(\frac{mn\pi^2}{w_1w_2})$, $O(\frac{m^2\pi^2}{w_2{}^2})$ and $O(\frac{n^2\pi^2}{w_1^2})$. It is second order term and maybe different in different situation.

From (2.4) and ignoring the second order terms, the approximate field above the ground is derived as

$$
\begin{aligned}
H_x &= \sum_{m,n=0}^{\infty}\frac{1}{i\omega\mu}\left\{-\lambda_{mn}b_{mn}\sin(\frac{n\pi x}{w_1})\cos(\frac{m\pi y}{w_2})\cos[\lambda_{mn}(z+d)]\right\}, (5.32)\\
H_y &= \sum_{m,n=0}^{\infty}\frac{1}{i\omega\mu}\left\{\lambda_{mn}a_{mn}\cos(\frac{n\pi x}{w_1})\sin(\frac{m\pi y}{w_2})\cos[\lambda_{mn}(z+d)]\right\}. \qquad (5.33)
\end{aligned}
$$

The next is focused on the integrals in (5.30) and (5.31). The new method is based on matching (5.30) with (5.32) and (5.31) with (5.33).

In three dimensional case, the kernel involves $\frac{1}{\sqrt{1-\xi_1^2-\xi_2^2}}$. Even though it is in L^1, it is less smooth at $\xi_1^2+\xi_2^2=1$.

Lemma 2.5.2.

$$
\int_{-1}^{1}\frac{\sin(\frac{x}{\epsilon})}{x}\frac{1}{\sqrt{1-x^2}}dx = \pi + O(\epsilon).
$$

Proof.

$$
\begin{aligned}
&\int_0^{1-\delta}\frac{\sin(\frac{x}{\epsilon})}{x}\frac{1}{\sqrt{1-x^2}}dx\\
\le\ &\int_0^{1-\delta}(1-\frac{1}{2}x^2)\frac{\sin(\frac{x}{\epsilon})}{x}dx\\
=\ & Si(\frac{1-\delta}{\epsilon}) - \frac{\epsilon^2}{2}(-\sin(\frac{1-\delta}{\epsilon}) + \frac{(1-\delta)\cos(w(1-\delta))}{\epsilon})\\
=\ & \frac{\pi}{2} + O(\epsilon)
\end{aligned}
$$

On the other hand,

$$
\begin{aligned}
& \int_{1-\delta}^{1} \frac{\sin(\frac{x}{\epsilon})}{x} \frac{1}{\sqrt{1-x^2}} dx \\
\leq & \int_{1-\delta}^{1} \frac{1}{x} \frac{1}{\sqrt{1-x^2}} dx \\
= & -\ln(\frac{1}{1-\delta} - \frac{\sqrt{1-(1-\delta)^2}}{1-\delta}) \\
= & O(\sqrt{\delta})
\end{aligned}
$$

if assume $\delta = O(\epsilon^2)$. Therefore the conclusion is correct. □

Lemma 2.5.3. *If $\frac{n\pi}{w} < 1$, then for any $a \in [0, w]$, the following is true.*

$$
\begin{aligned}
& \int_{-1}^{1} e^{iax} \frac{1}{\sqrt{1-x^2}} \left[\frac{\sin(w(x-\frac{n\pi}{w}))}{x-\frac{n\pi}{w}} - \frac{\sin(w(x+\frac{n\pi}{w}))}{x+\frac{n\pi}{w}} \right] dx \\
= & \ (Si(w-n\pi) + Si(w+n\pi)) \sin(\frac{n\pi a}{w}) \sqrt{1-(\frac{n\pi}{w})^2} + O(1/w).
\end{aligned}
$$

$$
\begin{aligned}
& \int_{-1}^{1} e^{iax} \frac{1}{\sqrt{1-x^2}} \left[\frac{\sin(w(x-\frac{n\pi}{w}))}{x-\frac{n\pi}{w}} + \frac{\sin(w(x+\frac{n\pi}{w}))}{x+\frac{n\pi}{w}} \right] dx \\
= & \ (Si(w-n\pi) + Si(w+n\pi)) \cos(\frac{n\pi a}{w}) \sqrt{1-(\frac{n\pi}{w})^2} + O(1/w), \\
& \int_{1}^{\infty} e^{iax} \frac{1}{\sqrt{1-x^2}} \left[\frac{\sin(w(x-\frac{n\pi}{w}))}{x-\frac{n\pi}{w}} - \frac{\sin(w(x+\frac{n\pi}{w}))}{x+\frac{n\pi}{w}} \right] = O(1/w), \\
& \int_{1}^{\infty} e^{iax} \frac{1}{\sqrt{1-x^2}} \left[\frac{\sin(w(x-\frac{n\pi}{w}))}{x-\frac{n\pi}{w}} + \frac{\sin(w(x+\frac{n\pi}{w}))}{x+\frac{n\pi}{w}} \right] = O(1/w).
\end{aligned}
$$

Proof. The latter two are easily seen from Riemann-Lebesgue theorem. The first two could be similarly proved as Lemma (1.4.3) □

Note that

$$
\int_{1}^{\infty} \int_{1}^{\infty} \frac{1}{\sqrt{x^2+y^2-1}} \frac{1}{x^2 y} dx dy < \infty
$$

when ξ_1 and ξ_2 are large enough, the Lebesgue dominant convergence theorem could be used to (5.31) with (5.33). Another fact used below is that

$$\int_a^\infty \frac{1}{\xi^2-(\frac{n\pi}{w})^2}(1-\cos w\xi)\sin(y\xi)d\xi = O(\frac{n\pi}{w})$$

for $a > 1$. This could be seen from Lebesgue dominant convergence theorem and

$$\begin{aligned}&\int_a^\infty \frac{1}{\xi^2-(\frac{n\pi}{w})^2}\sin(y\xi)d\xi\\ =\ & \frac{w}{2n\pi}\left\{\left[Si(\frac{y(n\pi-wa)}{w})+Si(\frac{y(n\pi+wa)}{w})\right]\cos(\frac{n\pi y}{w})\right.\\ &\left.-\left[Ci(\frac{y(n\pi-wa)}{w})+Ci(\frac{y(n\pi+wa)}{w})\right]\sin(\frac{n\pi y}{w})\right\}\end{aligned}$$

Even though there is a factor of $\frac{w}{2n\pi}$ in the anti-derivative, the following estimate could still be derived

$$\int_a^\infty \frac{1}{\xi^2-(\frac{n\pi}{w})^2}\sin(y\xi)d\xi = O(\frac{n\pi}{w})$$

by the usual taylor's expansion.

Lemma 2.5.4.

$$\begin{aligned}&\int_{R^2}\frac{[E_0(\sin\frac{n\pi x}{w_1}\cos\frac{m\pi y}{w_2})]^\wedge}{\sqrt{k_0^2-\xi_1^2-\xi_2^2}}e^{i(x\xi_1+y\xi_2)}d\xi\\ =\ & \left[\frac{(Si(w_1-n\pi)+Si(w_1+n\pi))^2}{2\pi}\frac{1}{\overline{\lambda}_{mn}}+\frac{1}{4\kappa\pi}gm(\kappa,y)\right.\\ +\ & \left.\frac{i}{4\kappa\pi}fn(\kappa,y)+\frac{i}{8k_0\pi}fn(k_0,x)gm(k_0,y)\right]\sin\frac{n\pi x}{w_1}\cos\frac{m\pi y}{w_2}+O(\frac{n\pi}{w})\end{aligned}$$

where $\kappa=\sqrt{k_0^2-(\frac{n\pi}{w_1})^2}$ *and*

$$\begin{aligned}&\int_{R^2}\frac{[E_0(\cos\frac{n\pi x}{w_1}\sin\frac{m\pi y}{w_2})]^\wedge}{\sqrt{k_0^2-\xi_1^2-\xi_2^2}}e^{i(x\xi_1+y\xi_2)}d\xi\\ =\ & [\frac{(Si(w_2-m\pi)+Si(w_2+m\pi))^2}{2\pi}\frac{1}{\overline{\lambda}_{mn}}+\frac{1}{4\kappa\pi}gm(\kappa,x)\\ +\ & \frac{i}{4\kappa\pi}fm(\kappa,x)+\frac{i}{8k_0\pi}fm(k_0,y)gm(k_0,x)\,]\cos\frac{n\pi x}{w_1}\sin\frac{m\pi y}{w_2}+O(\frac{n\pi}{w})\end{aligned}$$

where $\kappa = \sqrt{k_0^2 - (\frac{m\pi}{w_2})^2}$.

Proof. Let $h_n(x,w) = (1-(-1)^n e^{-iwx})/(x^2 - (\frac{n\pi}{w})^2)$, then

$$\int_{R^2} \frac{[E_0(\sin\frac{n\pi x}{w_1}\cos\frac{m\pi y}{w_2})]\hat{}}{\sqrt{k_0^2-\xi_1^2-\xi_2^2}} e^{i(x\xi_1+y\xi_2)} d\xi =$$

$$\begin{aligned} &= \frac{i}{2\pi}\frac{n\pi}{w}\int \xi_2[\Re(h_m(\xi_2,w_2)) + \Im(h_m(\xi_2,w_2))]e^{iy\xi_2}d\xi_2 \\ &\times \int [\Re(h_n(\xi_1,w_1)) + \Im(h_n(\xi_1,w_1))]\frac{1}{\sqrt{k_0^2-\xi_1^2-\xi_2^2}}e^{ix\xi_1}d\xi_1 \\ &\triangleq R_mR_n + R_mI_n + I_mR_n + I_mI_n \end{aligned}$$

Among these integrals, using Lemma (2.5.3)

$$I_mI_n = \frac{(Si(w-n\pi)+Si(w+n\pi))^2}{2\pi}\frac{1}{\lambda_{mn}}\sin\frac{n\pi x}{w_1}\cos\frac{m\pi y}{w_2} + R_1$$

Here R_1 takes one of the following forms: $O(\frac{m\pi}{w_2})$ and $O(\frac{n\pi}{w_1})$. It is first order term and maybe different in different situation.

$$R_mI_n = \frac{1}{4\kappa\pi}g_m(\kappa,y)\sin\frac{n\pi x}{w_1}\cos\frac{m\pi y}{w_2} + R_{ss}$$

where

$$\begin{aligned} g_m(\kappa,y) = \Big[&-2Si(\frac{y(n\pi-w\kappa)}{w}) + Si(\frac{(y+w)(n\pi-w\kappa)}{w}) \\ &-Si(\frac{(w-y)(n\pi-w\kappa)}{w}) - Si(\frac{(w+y)(n\pi+w\kappa)}{w}) \\ &+2Si(\frac{y(n\pi+w\kappa)}{w}) + Si(\frac{(w-y)(n\pi+w\kappa)}{w})\Big]. \end{aligned}$$

and $R_{ss}(x)$ are terms involving $\sin\frac{n\pi x}{w_1}\sin\frac{m\pi y}{w_2}$. They are not essential parts in the sense of L^2.

$$R_nI_m = \frac{i}{4\kappa\pi}f_n(\kappa,y)\sin\frac{n\pi x}{w_1}\cos\frac{m\pi y}{w_2} + R_{cc}$$

and $R_{cc}(x)$ is the term involving $\cos\frac{n\pi x}{w_1}\cos\frac{m\pi y}{w_2}$. f_n is defined in Chapter 1 (4.35).

$$R_mR_n = \frac{i}{8k_0\pi}f_n(k_0,x)g_m(k_0,y)\sin\frac{n\pi x}{w_1}\cos\frac{m\pi y}{w_2} + R_{cc} + R_{ss}$$

□

Using the boundary conditions, field representations and the above lemmas, two equations are obtained by matching (5.30) with (5.32) and (5.31) with (5.33). Together with (2.4)

$$\frac{n\pi}{w_1}a_n + \frac{n\pi}{w_2}b_n + \lambda_n c_n = 0$$

Therefore a_n, b_n and c_n are solvable. μ_1 and μ_2 are the permeabilities above the ground and below the ground plane, respectively.

2.6 Numerical Experiments

The first example is the calculation of the back scattering RCS for a long and narrow cavity ($w_1 = 2.5$, $w_2 = 0.25$, $d = 0.25$). Figure 2.3 presents the RCS for $\theta = 90^o$. The upper curve is for the H polarization and the lower cure is for the E polarization. Figure 2.4 shows the RCS for $\theta = 0$ in the case of the H polarization. The results are compared with the example in [21] and they agree well.

The second example is for a material-filled cavity with $w_1 = 1$, $w_2 = 0.25$, $d = 0.25$, $\epsilon_r = 7 + 1.5i$ and $\mu_r = 1.8 + 0.1i$. Figure 2.5 shows the RCS for $\phi = 90^o$. The continuous curve is for the H polarization and the dashed cure is for the E polarization. Figure 2.6 shows the RCS for $\phi = 0$ in the case of the H polarization. These curves agree well with the results in [21]. Figure 2.6 presents the back scattering RCS for the E polarization. The dashed line is for $\phi = 0$ and the continuous line is for $\phi = \pi/2$. They agree well with the results in [21], [23].

The third example is for a relatively deep cavity with $w_1 = 0.7$, $w_2 = 0.1$ and $d = 1.73$. In this case, $\theta = 40^o$. The continuous line in Figure 2.7 is the plot of σ_{EH}. The dashed line is the plot of σ_{HE}. They agree well with the results in [21], [23]. Finally, it should be pointed out that numerical studies are currently in progress,

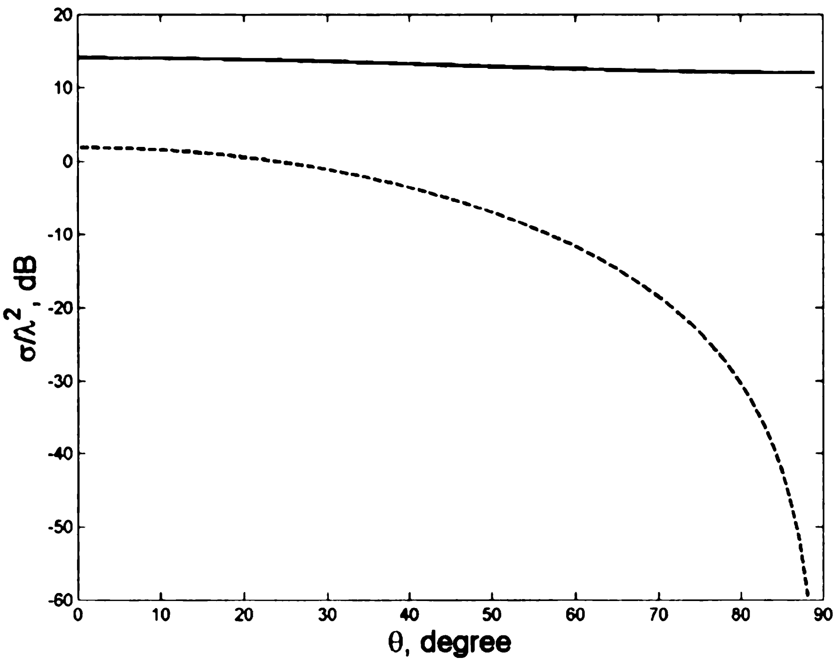

Figure 2.3. Improved mode matching method (ϕ=$\pi/2$).

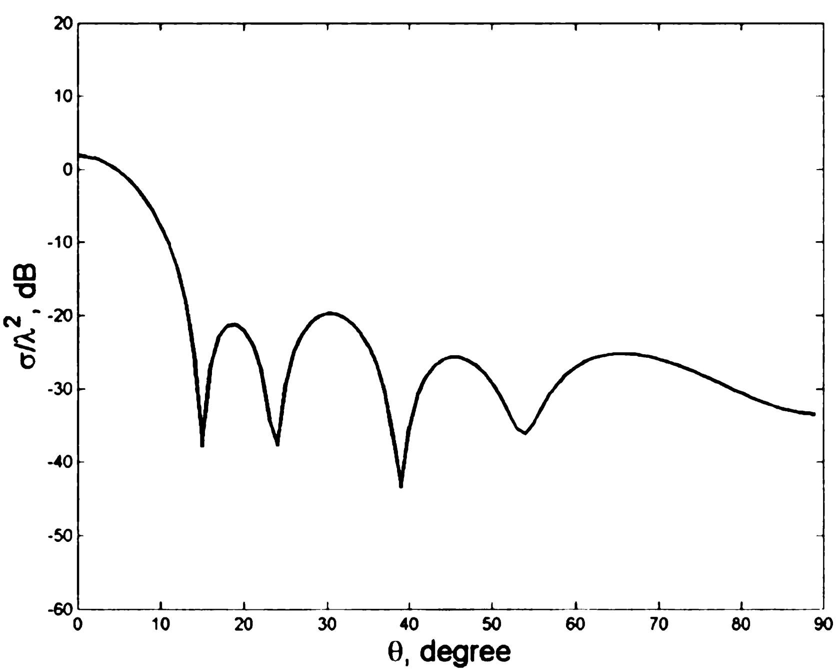

Figure 2.4. Improved mode matching method (ϕ=0).

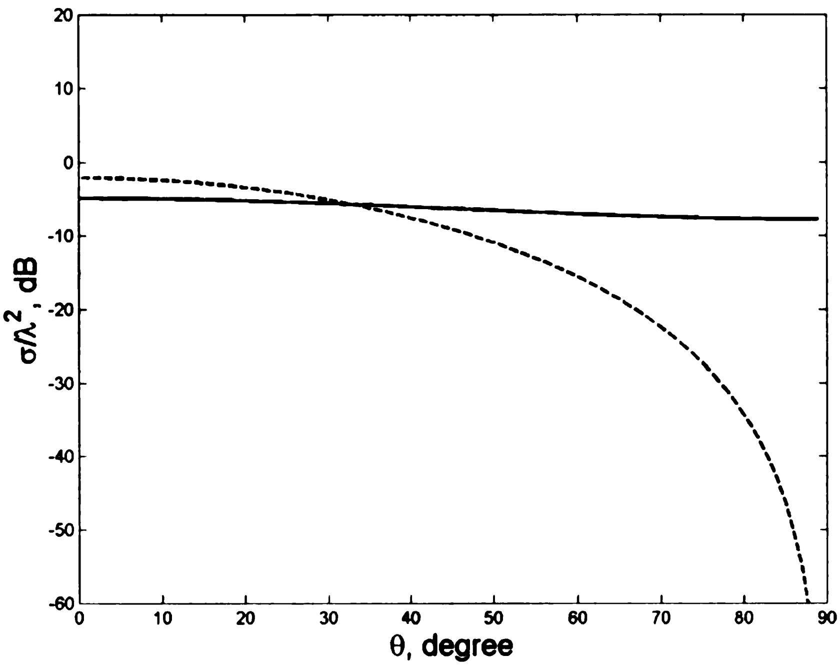

Figure 2.5. Improved mode matching method ($\phi=\pi/2$).

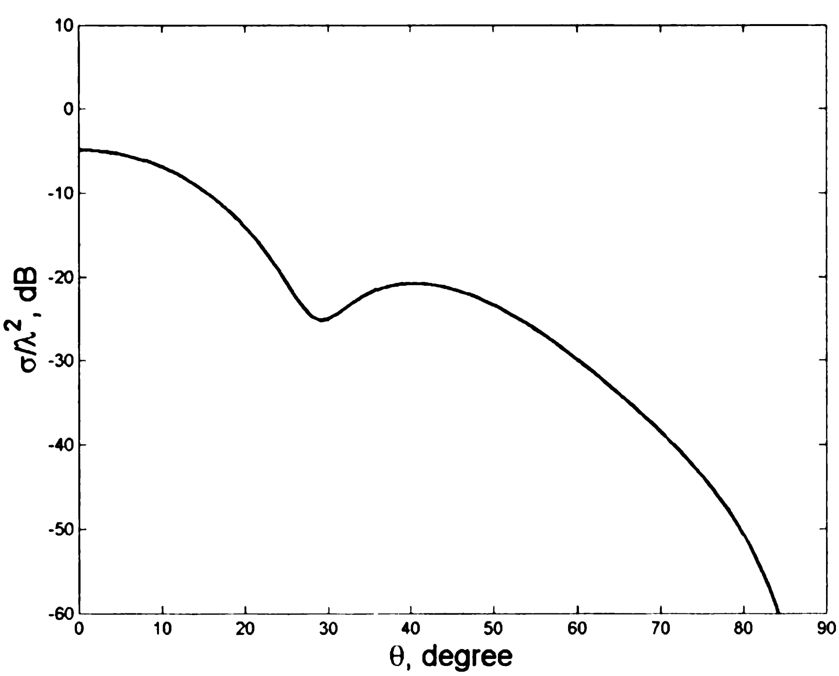

Figure 2.6. Improved mode matching method ($\phi=0$).

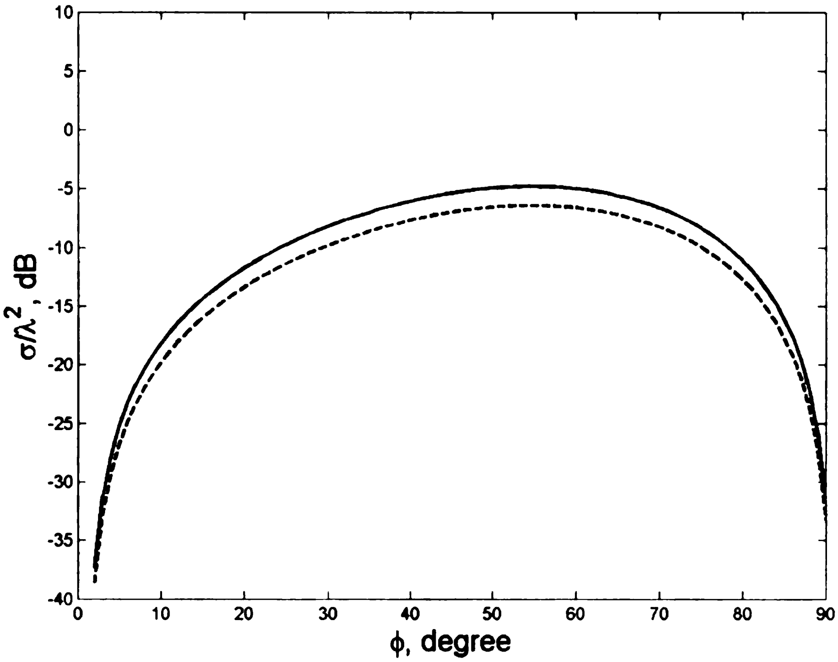

Figure 2.7. Improved mode matching method (θ=40^{o}).

especially in the co polarization RCS.

Appendix

Theorem 1 Suppose $\phi(x) \in C_0^{\infty}(R)$ and $\phi(x)$ is an even function, then

$$\int_{-\infty}^{\infty} \frac{\sin(\frac{x}{\epsilon})}{x}\phi(x)dx = \int_{-\infty}^{\infty} \delta(x)\phi(x)dx + O(\epsilon^3).$$

Proof Assume $supp(\phi) = [-1,1]$.

$$\frac{1}{2}\int_{-\infty}^{\infty} \frac{\sin(\frac{x}{\epsilon})}{x}\phi(x)dx = \int_0^{\frac{1}{\epsilon}} \frac{\sin y}{y}\left[\phi(0) + \sum_{n=1}^{\infty} \frac{\phi^{(2n)}(0)}{(2n)!}\epsilon^{2n}y^{2n}\right] dy$$

Collect the similar terms of ϵ^i,

$$\begin{aligned}
\epsilon^0: \quad & \phi(0)\frac{\pi}{2} = \frac{1}{2}\int_{-\infty}^{\infty} \delta(x)\phi(x)dx \\
\epsilon\cos(\frac{1}{\epsilon}): \quad & -\phi(0) - \sum_{n=1}^{\infty} \frac{\phi^{(2n)}(0)}{(2n)!} = -\sum_{n=0}^{\infty} \frac{\phi^{(2n)}(0)}{(2n)!} = -\phi(1) \\
\epsilon^2\sin(\frac{1}{\epsilon}): \quad & -\phi(0) + \sum_{n=1}^{\infty} \frac{\phi^{(2n)}(0)}{(2n)!}(2n-1) \\
& = -\sum_{n=0}^{\infty} \frac{\phi^{(2n)}(0)}{(2n)!} + \sum_{n=1}^{\infty} \frac{\phi^{(2n)}(0)}{(2n-1)!} = -\phi(1) + \phi'(1) \\
\epsilon^3\cos(\frac{1}{\epsilon}): \quad & 2\phi(0) + \sum_{n=2}^{\infty} \frac{\phi^{(2n)}(0)}{(2n)!}(2n-1)(2n-2) \\
& = \sum_{n=2}^{\infty} \frac{\phi^{(2n)}(0)}{(2n-2)!} - 2\sum_{n=1}^{\infty} \frac{\phi^{(2n)}(0)}{(2n-1)!} + 2\sum_{n=0}^{\infty} \frac{\phi^{(2n)}(0)}{(2n)!} \\
& = \phi''(1) - 2\phi'(1) + 2\phi(1) + \phi''(0)
\end{aligned}$$

Since $supp(\phi) \in [-1,1]$,

$$\int_{-\infty}^{\infty} \frac{\sin(\frac{x}{\epsilon})}{x}\phi(x)dx = \int_{-\infty}^{\infty} \delta(x)\phi(x)dx + \phi''(0)\epsilon^3\cos(\frac{1}{\epsilon}) + O(\epsilon^4).$$

Theorem 2 Suppose $\phi(x)$ satisfies the following assumptions,

(a) $\phi(x) \in C^{\infty}(R)$;

(b) $\phi(x) = 0$ for $x \in [-1,1]$;

(c) $\phi(x) = |x| \sum_{n=0}^{\infty} t_n \frac{1}{x^{2n}}$ for $|x| > 1$.

Then

$$\int_{-\infty}^{\infty} \frac{\sin(\frac{x}{\epsilon})}{x} \phi(x) dx = O(\epsilon).$$

Proof

$$\frac{1}{2} \int_{-\infty}^{\infty} \frac{\sin(\frac{x}{\epsilon})}{x} \phi(x) dx = \epsilon \int_{\frac{1}{\epsilon}}^{\infty} \sin y \sum_{n=0}^{\infty} t_n \frac{1}{(\epsilon y)^{2n}} dy$$

$$= \epsilon t_0 \cos(\frac{1}{\epsilon}) + \epsilon \sum_{n=1}^{\infty} t_n \Big[\cos \frac{1}{\epsilon} + 2n\epsilon \sin \frac{1}{\epsilon} - 2n(2n+1)\epsilon^2 \cos \frac{1}{\epsilon}$$

$$-2n(2n+1)(2n+2)\epsilon^3 \sin \frac{1}{\epsilon} \Big] + O(\epsilon^4)$$

$$= f(1)\epsilon \cos(\frac{1}{\epsilon}) + 2f'(1)\epsilon^2 \sin(\frac{1}{\epsilon}) - \epsilon^3 \cos(\frac{1}{\epsilon})[4f''(1) + 6f'(1)] + O(\epsilon^4)$$

Here $f(x) \in C^{\infty}$ and $f(x) = \sum_{n=0}^{\infty} t_n x^n$. Further, if $f(1) = f'(1) = f''(1) = 0$, then

$$\int_{-\infty}^{\infty} \frac{\sin(\frac{x}{\epsilon})}{x} \phi(x) dx = O(\epsilon^4).$$

BIBLIOGRAPHY

BIBLIOGRAPHY

[1] A. Altintas, P. H. Pathak and M. Liang, A selective Modal Scheme for the Analysis of EM Coupling Into or Radiation from Large Open-Ended Waveguides, IEEE Trans. Antennas Propagat, Vol. 36, No.1, Jan. 1988, pp. 84-96.

[2] H. Ammari G. Bao and A. Wood, A cavity problem for Maxwell's equations, Meth. Appl. Anal. 9, 2002, 249-260.

[3] H. Ammari, G. Bao and A.W. Wood, Analysis of the Electromagnetic Scattering from a Cavity, Japan J. Indust. Appl. Math., 19, 2002, pp. 301-310.

[4] G. Bao and J. Liu, Accurate Computation of the Electromagnetic Scattering from a Cavity, Proceedings of 3rd International Workshop on Scientific Computing and Applications, ed. by Y. Lu, W. Sun, and T. Tang, Sci. Press, Beijing, 45-54, 2004.

[5] G. Bao and W. Sun, A Fast Algorithm for the Electromagnetic Scattering from a Cavity, submitted.

[6] R.J. Burkholder and T. Lundin, Forward-Backward Iterative Physics Optical Algorithm for Computing the RCS of Open-ended Cavities, IEEE Trans. Antennas Propagat, Vol. 53 , 2 , Feb. 2005 pp. 793-799.

[7] R. F. Harrington, Time-Harmonic Electromagnetic Fields, Mcgraw-Hill College.

[8] J. Jin, The Finite Element Method in Electromagnetics, New York, Wiley, 1993.

[9] H. Liang, S. Lee and R. Chou, High-Frequency RCS of Open Cavities with Rectangular and Circular Cross Sections, IEEE Trans. Antennas Propagat, Vol. 37, No.5, may. 1989, pp. 648-654.

[10] M. A. Morgan, Mode Expansion Solution for Scattering by a Material Filled Rectangular Groove, Progress In Electromagnetics Research, Pier 18, 1998, pp. 1-17.

[11] H.H. Park and H.J. Eom, Electromagnetic Penetration into 2-D Multiple Slotted Rectangular Cavity: TM-wave Antennas and Propagation, IEEE Trans. Antennas Propagat, Vol. 48 , 2 , Feb. 2000 pp. 331-333.

[12] T. Van and A. W. Wood, Finite Element Analysis of Electromagnetic Scattering From a Cavity, IEEE Trans. Antennas Propagat, Vol. 51, No.1, Jan. 2003, pp. 130-137.

[13] B. Wei and D. Ge, Scattering by a Two-dimensional Cavity Filled with an Anisotropic Medium, Waves in Random Media, 13, 2003, pp. 223-240.

[14] Z. Xiang and T. Chia, IEEE Trans. Antennas Propagat, Vol. 49, No.2, Feb. 2001, pp. 165-173.

[15] S. Chandler-Wilde and B. Zhang, A uniqueness result for scattering by infinite rough surfaces, SIAM J. Appl. Math, Vol. 58, No. 6, pp. 1774-1790, 1998.

[16] C. R. Paul, K. W. whites, S. A. Nasar, Introduction to electromagnetic fields, third edition.

[17] L. C. Evans, Partial Differential Equations, AMS, Providence, Rhode Island

[18] S. N. Chandler-wilde and P. Monk, Existence, uniqueness and variational methods for scattering by unbounded rough surfaces, SIAM J. Math. Anal., Vol. 37, No. 2, pp. 598-618, 2005

[19] N. Bleistein, R. A. Handelsman and J. S. Lew, Functions whose fourier transforms decay at infinity: An Extensiton of the Riemann-Lebesgue Lemma, SIAM J. Math. Anal., Vol. 3, No. 3, pp. 485-495, 1972

[20] C. Gasquet and P. Witomski, Translated by R. Ryan, Fourier Analysis and Applications, Springer, 1998

[21] Electromagnetic Scattering Analysis of a three-dimensional-cavity-Backed Aperture in an infinite ground plane using a combined finite element method/method of moments approach, C. J. Reddy, M. D. Deshpande, C. R. Cockrell and F. B. Beck, NASA Technical Paper 3544, 1995

[22] Antenna Theory, Part 1, R. E. Collin and F. J. Zucker, McGraw-Hill Book Company, 1969

[23] K. Barkeshli and J. L. Volakis, Electromagnetic scattering from an aperture formed by a rectangular cavity recessed in a ground plane, J. Elec. Wave. Appl., VOl. 5, No. 7, 715-734, 1991